

# Role of H<sub>2</sub>O in Catalytic Conversion of C<sub>1</sub> Molecules

Lei Jiang,<sup>#</sup> Kongzhai Li,<sup>\*,#</sup> William N. Porter, Hua Wang, Gengnan Li,<sup>\*</sup> and Jingguang G. Chen<sup>\*</sup>



Cite This: *J. Am. Chem. Soc.* 2024, 146, 2857–2875



Read Online

ACCESS |

Metrics & More

Article Recommendations

**ABSTRACT:** Due to their role in controlling global climate change, the selective conversion of C<sub>1</sub> molecules such as CH<sub>4</sub>, CO, and CO<sub>2</sub> has attracted widespread attention. Typically, H<sub>2</sub>O competes with the reactant molecules to adsorb on the active sites and therefore inhibits the reaction or causes catalyst deactivation. However, H<sub>2</sub>O can also participate in the catalytic conversion of C<sub>1</sub> molecules as a reactant or a promoter. Herein, we provide a perspective on recent progress in the mechanistic studies of H<sub>2</sub>O-mediated conversion of C<sub>1</sub> molecules. We aim to provide an in-depth and systematic understanding of H<sub>2</sub>O as a promoter, a proton-transfer agent, an oxidant, a direct source of hydrogen or oxygen, and its influence on the catalytic activity, selectivity, and stability. We also summarize strategies for modifying catalysts or catalytic microenvironments by chemical or physical means to optimize the positive effects and minimize the negative effects of H<sub>2</sub>O on the reactions of C<sub>1</sub> molecules. Finally, we discuss challenges and opportunities in catalyst design, characterization techniques, and theoretical modeling of the H<sub>2</sub>O-mediated catalytic conversion of C<sub>1</sub> molecules.

## 1. INTRODUCTION

Water (H<sub>2</sub>O) is intimately related to numerous chemical reactions. In living organisms, almost all chemical reactions take place in aqueous medium. H<sub>2</sub>O plays the role of solvent, reactant, byproduct, catalyst, and proton transfer agent. For a long time, the understanding of H<sub>2</sub>O has been mainly limited to its role as a reaction medium, while knowledge of other functions of H<sub>2</sub>O in chemical reactions is insufficient.<sup>1,2</sup> With the development of experimental detection techniques and advancements in computational chemistry, the structure and dynamics of H<sub>2</sub>O molecules have been studied at the molecular level to investigate the multifaceted effects of water on chemical reactions.<sup>3–6</sup>

Apart from its well-known role as a solvent or an intentionally added component, the presence of H<sub>2</sub>O is often unavoidable in other nonaqueous environments. For example, H<sub>2</sub>O molecules may be present in reactants or products adsorbing on the surfaces of catalysts.<sup>7,8</sup> Its presence is frequently identified as a destructive factor that shortens the lifetime of catalysts, reduces the production of desired compounds, reacts with intermediates and products to cause side reactions, and influences the performance of working catalysts.<sup>9–11</sup> On the other hand, numerous cases have demonstrated that H<sub>2</sub>O can play a role as a participant or promoter,<sup>12–17</sup> supply or stabilize highly reactive species,<sup>18–20</sup> create a microscale solvation environment,<sup>21–23</sup> and enhance reaction rates and product selectivity in heterogeneous catalysis. These effects are especially important for gaseous phase reactions, including a variety of transformations to upgrade C<sub>1</sub> molecules such as CH<sub>4</sub>, CO, and CO<sub>2</sub> that can enable the production of value-added chemicals from inexpensive feedstocks.

The effects of H<sub>2</sub>O in catalytic reactions have been highlighted in several recent Reviews and Perspective

articles.<sup>6,24</sup> Resasco et al. provided a review on the H<sub>2</sub>O-mediated heterogeneously catalyzed reactions of primarily large hydrocarbons and biomass-derived molecules.<sup>25</sup> Ma and co-workers focused on catalytic reactions that occur in the aqueous phase, including alcohol or biomass-derived polyol reforming, CH<sub>4</sub> activation, and other C<sub>1</sub> reactions.<sup>26</sup> The present article is devoted to providing a perspective on H<sub>2</sub>O-mediated thermocatalytic conversion of gaseous C<sub>1</sub> molecules including CO<sub>2</sub>, CO, and CH<sub>4</sub>. Specifically, in this Perspective, we briefly review the state and function of H<sub>2</sub>O in catalytic reactions involving C<sub>1</sub> molecules that occur mainly in the gaseous phase. We will then discuss the promoting effects of H<sub>2</sub>O in these reactions and various methods to overcome the negative effects of H<sub>2</sub>O. We will also discuss challenges and future opportunities in catalyst design, characterization techniques, and theoretical modeling of the H<sub>2</sub>O-mediated catalysis of C<sub>1</sub> molecules.

## 2. H<sub>2</sub>O AS A PROMOTOR OR COREACTANT IN CO REACTIONS

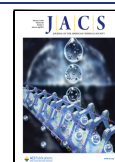
**2.1. Water–Gas Shift Reaction.** As one of the most important reactions to produce hydrogen in the energy and chemical industries, the water–gas shift (WGS) reaction (CO + H<sub>2</sub>O → H<sub>2</sub> + CO<sub>2</sub>, ΔH<sup>0</sup> = –41 kJ/mol) has been widely studied. In addition, the WGS reaction and its reverse reaction are directly or indirectly relevant to other catalytic systems relying on the coexistence of H<sub>2</sub>O with CO, H<sub>2</sub>, or CO<sub>2</sub>,

**Received:** November 28, 2023

**Revised:** December 27, 2023

**Accepted:** December 28, 2023

**Published:** January 24, 2024



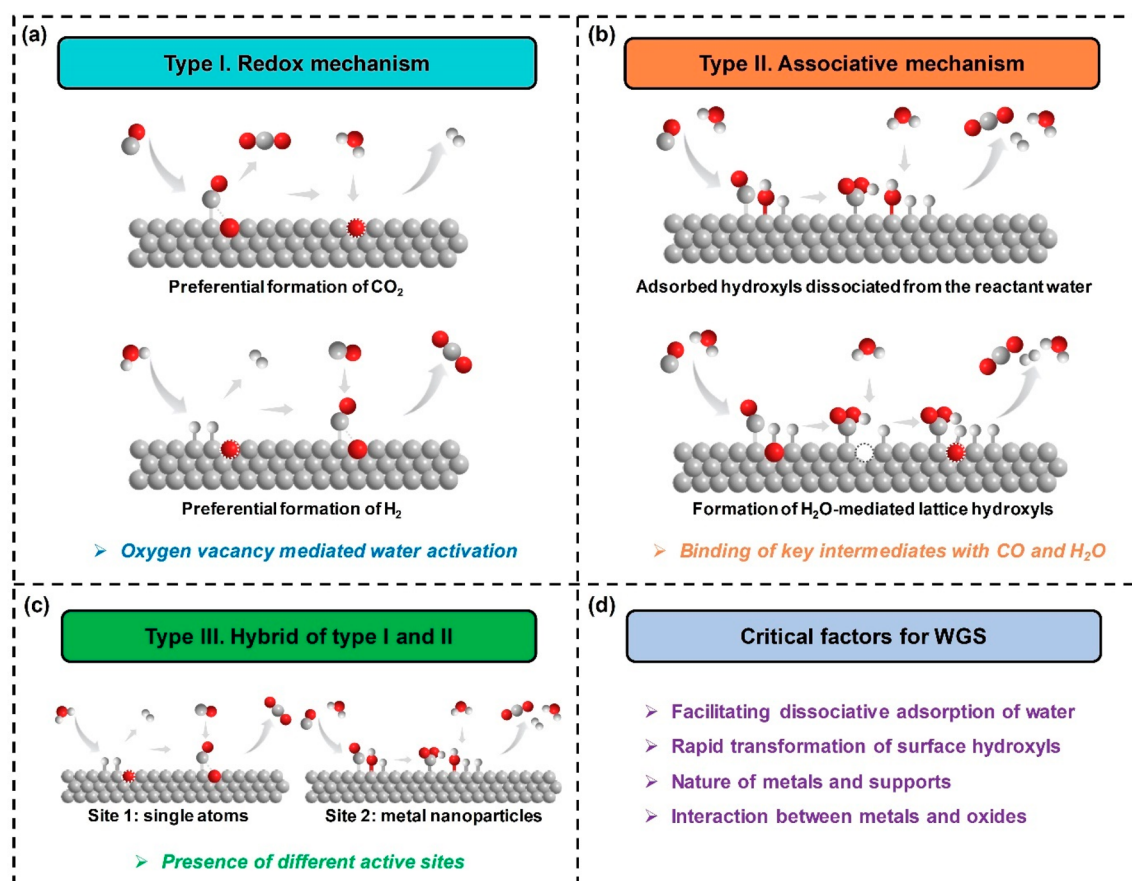


**Figure 1.** A summary of reaction mechanisms in the water–gas shift reaction. (a) Type I: redox mechanism. (b) Type II: associative mechanism. (c) Hybrid mechanism of types I and II. (d) Critical factors for the water–gas shift reaction.

including methanol synthesis, Fischer–Tropsch synthesis, methanol steam reforming, and coal gasification. Therefore, understanding the role of H<sub>2</sub>O in the WGS reaction is also beneficial for clarifying the reaction mechanisms of the above-mentioned reactions.

Two types of reaction mechanisms are typically considered for the WGS reaction: the redox or regenerative mechanism and the associative mechanism (Figure 1).<sup>27,28</sup> For the redox mechanism, it has been proposed that an adsorbed CO molecule reacts with an activated oxygen atom from the catalyst to produce CO<sub>2</sub>, generating an oxygen vacancy site. The reduced catalyst is then replenished by H<sub>2</sub>O dissociation, leading to the formation of H<sub>2</sub>. In the associative mechanism, adsorbed CO is consumed by reacting with OH from H<sub>2</sub>O dissociation to generate carboxyl (COOH\*) or formate (HCOO\*) species as key intermediates. Though the precise mechanism is a matter of intense debate, both mechanisms involve a water dissociation step that is generally regarded as energetically important and, in some cases, as the rate-determining step (RDS).<sup>27,29–31</sup>

Regarding the redox mechanism (Figure 1a), one debate is focused on the reaction sequence of H<sub>2</sub>O dissociation and CO conversion.<sup>32</sup> The oxygen species responsible for the conversion of surface-adsorbed CO to CO<sub>2</sub> can be derived from the surface lattice oxygen of the catalysts, and the subsequent oxygen vacancies provide active sites for H<sub>2</sub>O dissociation, resulting in the formation of CO<sub>2</sub> before H<sub>2</sub>.<sup>33</sup> In contrast, H<sub>2</sub>O may first be activated on the catalyst surface to generate H<sub>2</sub> and reactive oxygen species, which then react with

the adsorbed CO to form CO<sub>2</sub>, resulting in the production of H<sub>2</sub> before CO<sub>2</sub>.<sup>34,35</sup> Moreover, for supported metal catalysts, interfacial bifunctional sites (M<sub>1</sub>–O<sub>v</sub>–M<sub>2</sub>) have also been proposed, in which CO is adsorbed on the metal site and H<sub>2</sub>O undergoes dissociation on the oxygen vacancies of the oxide support, followed by the subsequent reaction between adsorbed CO and the dissociated species at the metal–oxide interface.<sup>28,32,36,37</sup>

It is reported that the dissociation of H<sub>2</sub>O on a defective oxide surface is more thermodynamically preferred than on a well-defined oxide surface.<sup>27,31</sup> The nature of oxide supports (e.g., TiO<sub>x</sub>, CeO<sub>x</sub>, FeO<sub>x</sub> and Al<sub>2</sub>O<sub>3</sub>), which strongly affect the presence of oxygen vacancies, plays an important role. A comparative study on Au/Al<sub>2</sub>O<sub>3</sub> and Au/TiO<sub>2</sub> catalysts shows that H<sub>2</sub>O bonds weakly at the Au–Al<sub>2</sub>O<sub>3</sub> interface, while a much stronger binding for H<sub>2</sub>O is observed on the Au/TiO<sub>2</sub> catalyst due to the presence of oxygen vacancies.<sup>38</sup> As a result, the reaction rate per total mole of Au for Au/TiO<sub>2</sub> is 20 times higher than that for Au/Al<sub>2</sub>O<sub>3</sub>. The reduced apparent activation energy of H<sub>2</sub>O dissociation on Au/TiO<sub>2</sub> demonstrates that the oxide support is directly involved in the activation of H<sub>2</sub>O.<sup>38</sup> In addition, an investigation on the Au@TiO<sub>2-x</sub>/ZnO catalyst with a TiO<sub>2-x</sub> overlayer on the surface of Au nanoparticles using *Quasi in situ* X-ray photoelectron spectroscopy (XPS), *in situ* extended X-ray absorption fine structure (EXAFS), and *in situ* diffuse reflectance infrared Fourier transform spectroscopy (DRIFTS) confirms that both the electron-enriched Au<sup>δ-</sup> species and oxygen vacancies directly participate in the dissociation of H<sub>2</sub>O.<sup>39</sup> Similar

observations have also been reported on Ni/TiO<sub>2-x</sub>, Au/CeO<sub>2-x</sub>, and Ir/FeO<sub>x</sub> catalysts.<sup>31,35,36</sup>

In the case of the associative mechanism (Figure 1b), the hydroxyl groups from the dissociation of H<sub>2</sub>O play an important role.<sup>40</sup> The OH species originating from H<sub>2</sub>O alter the adsorption or readsorption behavior of reactants or products, leading to significant differences in the WGS activity and selectivity. Results from theoretical calculations indicate that wetting of the catalyst is controlled by the presence of OH groups on the surface, acting as anchors for water adsorption.<sup>41</sup> Moreover, favorable hydrogen bonding interactions stabilize the Zundel cations (H<sub>5</sub>O<sub>2</sub><sup>+</sup>) adsorbed on metal clusters and weaken the O–H bonds of adsorbed H<sub>2</sub>O, thereby exhibiting a lower energy pathway for H<sub>2</sub>O dissociation.<sup>34</sup> In addition to influencing the adsorption step, the OH species can also participate by reacting with CO to form carboxyl or formate intermediates. By comparing a density functional theory (DFT)-based microkinetic model with experimental reaction rates, Gokhale et al.<sup>30</sup> reported that the dissociative adsorption of H<sub>2</sub>O is the RDS for the WGS reaction on the Cu(111) surface. Compared with formate, which tends to block active sites, carboxyl is a more reactive intermediate. It reacts with an adjacent OH group on the Cu(111) surface, forming CO<sub>2</sub> and H<sub>2</sub>O (COOH\* + OH\* → CO<sub>2</sub>\* + H<sub>2</sub>O\*). Therefore, H<sub>2</sub>O in the WGS reaction not only reacts with CO to form CO<sub>2</sub> and H<sub>2</sub> but also acts as a promoter to facilitate the reaction due to the formation of adsorbed OH\* groups.<sup>30</sup> Likewise, by using *in situ* DRIFTS, Fu et al.<sup>31</sup> reported that the bridging-OH groups formed on the surface oxygen vacancies of the CeO<sub>2</sub> support are the key reactive species for the WGS reaction on Au-CeO<sub>2</sub> catalysts. The abundant Au-CeO<sub>2</sub> interfacial sites effectively promote the reaction between adsorbed CO on Au and bridging-OH groups formed on CeO<sub>2</sub>. For larger Au nanoparticles supported on CeO<sub>2</sub>, the limited number of interfacial sites leads to insufficient CO adsorption and thus weaker reactivity with the bridging-OH groups.<sup>31</sup> It is also proposed that there is a competitive adsorption of CO<sub>2</sub> and H<sub>2</sub>O on the surface of the catalysts, and the accumulation of surface carbonates blocks the active sites.<sup>42</sup> A facile reaction between the hydroxyl groups and the carbonate layer on the catalyst surface can prevent carbonate species from blocking the active sites.<sup>42</sup>

Similarly, preadsorbed H<sub>2</sub>O or cofed H<sub>2</sub>O can readily form surface hydroxyls on carbide catalysts.<sup>40,43,44</sup> For example, Ma and co-workers reported Au/ $\alpha$ -MoC catalysts for low-temperature WGS reaction, where the  $\alpha$ -MoC support facilitates the epitaxial growth of Au layers with altered electronic structures, which facilitate bonding with CO.<sup>44</sup> At a temperature of 303 K, H<sub>2</sub>O is activated on  $\alpha$ -MoC, and CO adsorbed on adjacent Au sites readily reacts with surface hydroxyl groups formed by H<sub>2</sub>O decomposition.<sup>44</sup> However, when the adsorbed hydroxyl species cannot be promptly converted, there is a problem of deep oxidation of  $\alpha$ -MoC during long-term catalytic processes, leading to catalyst deactivation. By adding Pt clusters and Pt single atoms, the excess surface active oxygen species can be eliminated, enhancing the stability toward WGS.<sup>43</sup>

It should be highlighted that the WGS reaction may occur simultaneously via both the redox mechanism and the associative mechanism, and the dominant pathway relies on the ability of the catalysts to facilitate H<sub>2</sub>O dissociation (Figure 1c). Chen et al.<sup>45</sup> compare the activity of Pt/FeO<sub>x</sub> catalysts with exclusively either Pt nanoparticles or single atoms for the WGS reaction and find that Pt nanoparticles accomplish the

WGS process through an associative mechanism, with CO strongly adsorbing on the Pt nanoparticle sites and reacting with the OH\* species generated by activation of H<sub>2</sub>O on the FeO<sub>x</sub> sites to form the formate intermediate. In contrast, Pt single atoms promote the formation of oxygen vacancies on FeO<sub>x</sub> that dissociate H<sub>2</sub>O to H<sub>2</sub> and adsorbed O, which then combines with the weakly adsorbed CO on the Pt sites to produce CO<sub>2</sub>.

In summary, regardless of the reaction pathways, fundamental factors controlling water dissociation and subsequent conversion are closely related to the geometric and electronic structures of the oxide supports and metal components in WGS catalysts.<sup>37</sup> Strong interactions between the metal species and the support may promote the formation of unique interfacial sites for optimizing the catalytic performance for the WGS reaction.<sup>36,39,46,47</sup>

**2.2. CO Oxidation.** Due to the limited activities of the current WGS catalysts in commercial processes, approximately 0.5–1.0 vol % of unconverted CO remains in the H<sub>2</sub> stream, which can poison the catalysts in their subsequent utilization in hydrogen fuel cells or ammonia synthesis. Therefore, preferential oxidation of CO in the H<sub>2</sub>-rich stream with the presence of H<sub>2</sub>O plays an important role in the H<sub>2</sub> purification step for various applications.<sup>48</sup> Similar to the WGS reaction, the presence of H<sub>2</sub>O in the feed gases modifies the catalytic activity for the CO oxidation reaction.<sup>12</sup>

Using a commercial Au/Al<sub>2</sub>O<sub>3</sub> catalyst as an example, Saavedra et al.<sup>49</sup> reported that the selectivity of CO oxidation in the presence of H<sub>2</sub> can be optimized by controlling the coverage of water on the catalyst surface. Generally, preferential CO oxidation (PROX) selectivity increases with the partial pressure of water since H<sub>2</sub>O has a more significant effect on blocking the sites for hydrogen adsorption than those for CO adsorption. As a result, with increasing H<sub>2</sub>O partial pressure, the H<sub>2</sub> oxidation is inhibited, and a higher selectivity of CO oxidation is observed when the catalyst surface is covered by one to two monolayers of water. However, a further increase in the water partial pressure typically leads to the deactivation of the catalyst.

In addition to the PROX for H<sub>2</sub> purification, the role of H<sub>2</sub>O in low temperature CO oxidation for emissions control has been extensively studied.<sup>15,50,51</sup> Depending on the catalyst used, H<sub>2</sub>O can be either an inhibitor or a promoter. For noble metal catalysts, a trace amount of H<sub>2</sub>O in the reactant feed stream is found to improve the CO oxidation activity by up to several orders of magnitude.<sup>51–53</sup> Many mechanistic questions regarding the role of H<sub>2</sub>O in the CO oxidation reaction have been raised in the past two decades, which include: (i) whether gaseous H<sub>2</sub>O directly participates in the formation of CO<sub>2</sub>; (ii) whether the reaction occurs through the Mars–van-Krevelen (MvK) or the Langmuir–Hinshelwood (LH) mechanism; and (iii) whether the reaction pathways involve intermediates such as carboxyl, carbonate, or bicarbonate.<sup>54–63</sup>

For example, the catalytic activity of Au/TiO<sub>2</sub> under H<sub>2</sub>O concentrations of 3–10 ppm has been observed to be about 10 times higher than under a dry condition (0.1 ppm). The reaction rate further increases with rising H<sub>2</sub>O concentration, reaching a maximum at 200 ppm.<sup>52</sup> On the other hand, the presence of excessive H<sub>2</sub>O can cover the active center of the catalyst, leading to a decrease in catalytic efficiency.<sup>52,64</sup> It has also been found that the influence of H<sub>2</sub>O on the activity of Au catalysts strongly depends on the type of oxide (CeO<sub>2</sub>, Fe<sub>2</sub>O<sub>3</sub>, TiO<sub>2</sub>, Al<sub>2</sub>O<sub>3</sub>, SiO<sub>2</sub>).<sup>49,53,59,65–69</sup> As shown in Figure 2a,b, Al<sub>2</sub>O<sub>3</sub>

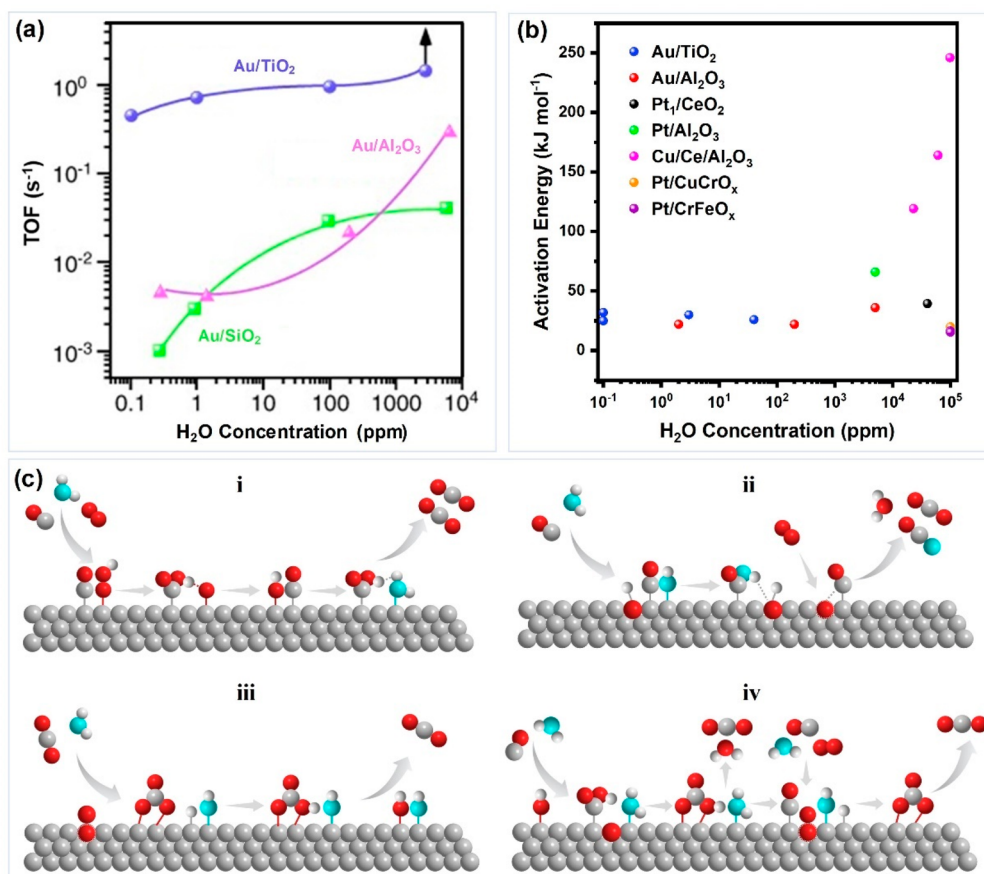


**Figure 2.** (a) Turnover frequencies (TOF) per surface gold atom at 273 K for CO oxidation over Au/TiO<sub>2</sub>, Au/Al<sub>2</sub>O<sub>3</sub>, and Au/SiO<sub>2</sub> as a function of H<sub>2</sub>O concentration. Upright arrow indicates the saturation of the CO conversion. Reproduced with permission from ref 53. Copyright 2004 Wiley. (b) A comparison of activation energy of CO oxidation catalysts in the presence of H<sub>2</sub>O. Data originated from refs 52, 53, 61, 64, 70, 71. (c) Proposed reaction mechanism of the CO oxidation in the presence of H<sub>2</sub>O.

seems more sensitive to the concentration of H<sub>2</sub>O than others, while the apparent activation energy of CO oxidation appears to have little correlation with H<sub>2</sub>O concentration for noble metal catalysts supported on other oxides.<sup>52,53,61,64,70,71</sup>

In general, it is accepted that the amount of H<sub>2</sub>O adsorbed on the catalyst, rather than the H<sub>2</sub>O concentration in the reactant feed, affects the activity.<sup>52–54</sup> Some H<sub>2</sub>O-derived species on the catalyst surface are speculated to activate molecular oxygen and promote the dissociation of carbonate to avoid deactivation.<sup>20,72–74</sup> In the absence of H<sub>2</sub>O, CO oxidation requires three steps: CO + O<sub>2</sub> → *cis*-OCOO\* → *trans*-OCOO\* → CO<sub>2</sub> + O\*. The adsorption of trace amounts of H<sub>2</sub>O near the active sites can facilitate the activation of oxygen, which is considered to be one of the RDS in CO oxidation. Saavedra et al.<sup>18,68</sup> have systematically investigated the mechanism of CO oxidation in the presence of H<sub>2</sub>O over TiO<sub>2</sub> or Al<sub>2</sub>O<sub>3</sub>-supported Au catalysts using Infrared (IR) spectroscopy, kinetic experiments, and DFT calculations (Figure 2c-i). The weakly adsorbed H<sub>2</sub>O on the catalyst surface increases the effective number of active centers without changing the intrinsic reactivity, and the coverage of H<sub>2</sub>O largely determines the catalytic activity.<sup>68</sup> For H<sub>2</sub>O-mediated O<sub>2</sub> activation, the barrier for O–O bond scission is reduced by 0.4 eV due to the formation of OOH\* via proton transfer, which helps activate O<sub>2</sub> at low temperatures.<sup>62</sup> The interaction of CO\* with OOH\* to generate COOH\* is more favorable than the interaction between CO\* and surface OH\*.<sup>18</sup>

Therefore, weakly adsorbed H<sub>2</sub>O is the key proton (H\*) donor. In these studies, neither the H<sub>2</sub>O nor the lattice oxygen of the oxide support is directly involved in CO<sub>2</sub> production at low temperatures on either reducible or inert oxides, and the rate enhancement mainly follows the H<sub>2</sub>O-mediated LH reaction mechanism.

Carbonate accumulation on the catalyst surface can also lead to a decrease in CO oxidation performance due to the blockage of active sites by carbonate.<sup>56</sup> Further conversion of carbonate to bicarbonate can be promoted by proton transfer through an H-bonded H<sub>2</sub>O network at the catalyst surface (Figure 2c-iii), which significantly reduces the activation barrier for CO<sub>2</sub> desorption from 1.5 to 0.6 eV.<sup>62</sup> A mechanism involving the presence of carbonate/bicarbonate intermediates and surface hydroxyl groups that enhance the rate has been proposed (Figure 2c-iv).<sup>56</sup> Specifically, surface hydroxyl groups drive the formation of carboxyl groups from CO, which are oxidized to bicarbonate by surface lattice oxygen and then decomposed to CO<sub>2</sub> and H<sub>2</sub>O by reacting with H atoms produced from H<sub>2</sub>O dissociation.

On the other hand, H<sub>2</sub>O has also been proposed to play a promotional role by directly participating in the CO oxidation at low temperature (77 K).<sup>57,58</sup> The formation of hydroxyl groups through oxygen activation by H\* produced from H<sub>2</sub>O and its reaction with adsorbed CO to form CO<sub>2</sub> has been observed using an ultrahigh vacuum (UHV) scattering/analysis chamber and DFT calculations, which is similar to the results

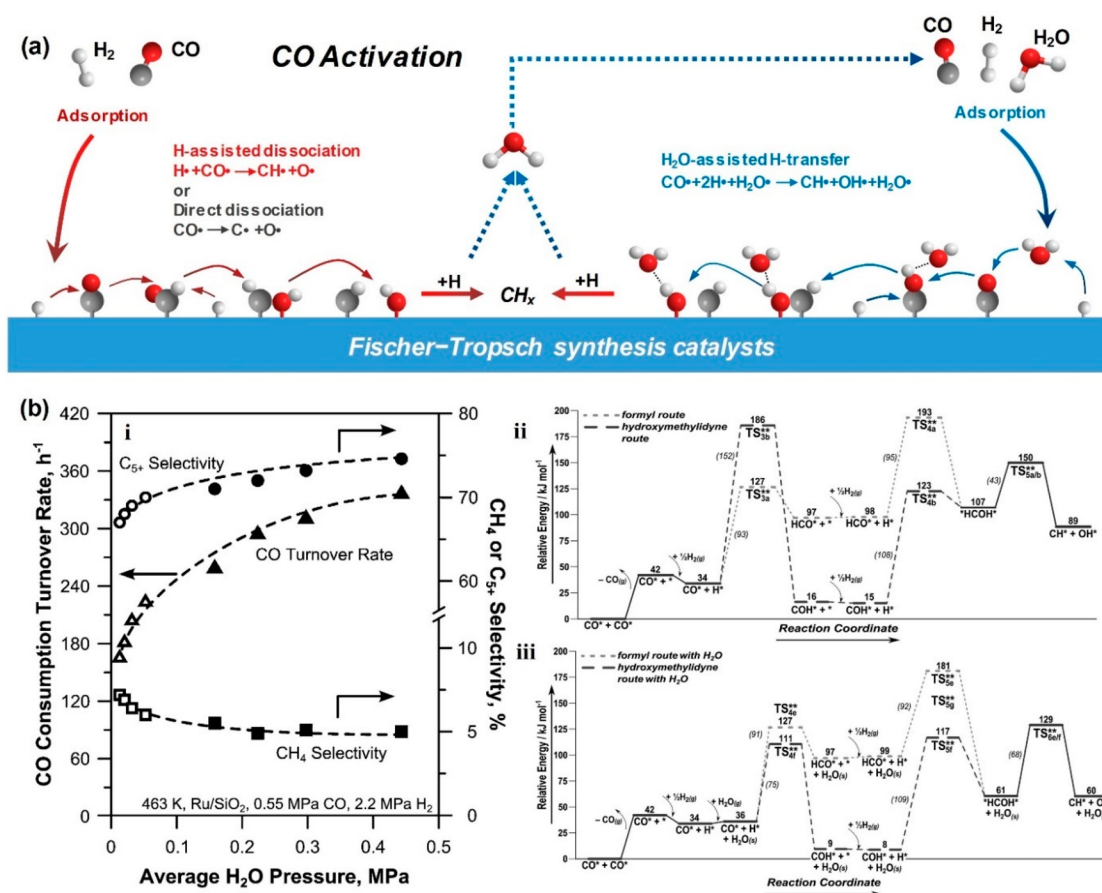


**Figure 3.** (a) Different mechanisms of CO activation on FTS catalysts. (b) Mechanistic role of H<sub>2</sub>O on the rate and selectivity of FTS on Ru catalysts: (i) CO consumption rate ( $\Delta$  or  $\blacktriangle$ ), CH<sub>4</sub> selectivity ( $\square$  or  $\blacksquare$ ), and C<sub>5+</sub> selectivity ( $\circ$  or  $\bullet$ ) as a function of H<sub>2</sub>O partial pressure on 5 wt % Ru/SiO<sub>2</sub> with a feed gas of H<sub>2</sub>/CO = 4.5. Open symbols: conversion changes; closed symbols: H<sub>2</sub>O addition; reaction coordinate diagrams for (ii) H-assisted CO activation via the formyl and hydroxymethylidyne routes in absence of H<sub>2</sub>O, (iii) H<sub>2</sub>O-mediated formyl and hydroxymethylidyne routes in the presence of H<sub>2</sub>O. Reproduced with permission from ref 89. Copyright 2013 Wiley.

using single-atom catalysts.<sup>71</sup> Specifically, the hydroxyl groups from dissociated H<sub>2</sub>O on the single atom Pt<sub>1</sub>/CeO<sub>2</sub> catalyst react with adsorbed CO to form a highly reactive carboxyl intermediate, which is dehydrogenated with the assistance of hydroxyl groups to generate CO<sub>2</sub> and H<sub>2</sub>O (Figure 2c-ii).<sup>61</sup> Such a pathway is more facile than the direct reaction of CO with the lattice oxygen, resulting in higher activity for CO oxidation.<sup>61</sup> On the other hand, Zhao et al. find that CeO<sub>2</sub>-supported single Au atoms are more effective as an electron acceptor, offering a more efficient channel for the CO + OH reaction pathway in the presence of OH groups from water dissociation.<sup>75</sup>

**2.3. Fischer–Tropsch Synthesis.** Fischer–Tropsch synthesis (FTS) is another important catalytic reaction in industry that converts syngas (a mixture of CO and H<sub>2</sub>) to value-added chemicals (hydrocarbons, oxygenates, etc.). The FTS reaction can be catalyzed using Fe-, Co-, and Ru-based materials.<sup>76–78</sup> H<sub>2</sub>O is an inherent byproduct in FTS as one H<sub>2</sub>O molecule is generated for each molecule of CO that is converted. H<sub>2</sub>O produced or cofed with the syngas reactants has a significant effect (either positive or negative) on the reaction rate, hydrocarbon selectivity, FTS product distribution, and catalyst longevity due to its influence on the degree of syngas adsorption on the catalyst, chain initiation, chain growth, methanation, hydrogenation to paraffins, and dehydrogenation to olefins.<sup>79</sup>

Early studies have reported that the influence of H<sub>2</sub>O is positive on unsupported and SiO<sub>2</sub>-supported cobalt oxide catalysts, negative for Al<sub>2</sub>O<sub>3</sub>-supported catalysts, and slightly beneficial for TiO<sub>2</sub>-supported catalysts.<sup>79–82</sup> These different H<sub>2</sub>O effects are attributed to three aspects: oxidation of the Co catalyst, removal of transport restrictions via the formation of an H<sub>2</sub>O-rich intrapellet liquid, and kinetic effects. Several mechanistic explanations have been offered to explain the influence of H<sub>2</sub>O in FTS. One hypothesis is that higher H<sub>2</sub>O partial pressure suppresses hydrogenation reactions at the surface by occupying sites for H<sub>2</sub> dissociation.<sup>83</sup> For Co/SiO<sub>2</sub> catalysts, increased reaction rates are due to the influence of H<sub>2</sub>O on the active species distribution on the Co surface,<sup>80</sup> and adsorbed H<sub>2</sub>O accelerates the CO dissociation rate with subsequent formation of CH<sub>x</sub> monomers.<sup>84,85</sup> Coadsorbed H<sub>2</sub>O presumably interacts with CO and lowers the energy barrier for CO activation. An increase in C<sub>5+</sub> products is associated with an increased coverage of reactive monomer species due to an increased polymerization rate without a simultaneous effect on termination probability. Fischer et al.<sup>86</sup> have proposed the possibility of H<sub>2</sub>O-induced changes on the active sites responsible for chain growth, or an inhibiting effect of H<sub>2</sub>O on methanation sites. H<sub>2</sub>O increases the amount of active surface carbon, which is present predominantly as a monomeric species. This increased surface concentration of monomeric carbon is caused by an acceleration of the CO

dissociation rate without a corresponding activity increase of the downstream hydrocarbon synthesis steps.<sup>83,87</sup> Therefore, the proposed monomer dependencies in the FTS mechanism explain the lower methane selectivity and higher molecular weight products observed at increased H<sub>2</sub>O concentrations.<sup>84,88</sup>

H-assisted pathways in kinetically relevant CO dissociation steps have also been proposed on both Fe and Co catalysts.<sup>90</sup> In such pathways, chemisorbed H\* and CO\* react to produce CH<sub>x</sub>O species, which dissociate to form OH\*. This leads to the preferential rejection of the O atoms in CO to produce H<sub>2</sub>O. These assisted pathways are the exclusive CO activation routes on Co catalysts and the predominant ones on Fe catalysts. They happen concurrently with unassisted CO dissociation on Fe-based catalysts, wherein rejected oxygen leaves are treated as CO<sub>2</sub> (Figure 3a).

Compared to Co-based catalysts, the effect of H<sub>2</sub>O on the performance of Fe-based FTS catalysts is more complicated due to the simultaneous occurrence of the WGS reaction, which is less significant on Co-based catalysts.<sup>91</sup> The WGS reaction consumes CO along with H<sub>2</sub>O produced during the FTS reaction to generate CO<sub>2</sub> and additional H<sub>2</sub>. Therefore, for Fe-based catalysts, the addition of H<sub>2</sub>O to the syngas feed affects the partial pressure of CO and H<sub>2</sub> inside the reactor by increasing the WGS rate. Karn et al.<sup>92</sup> reported that the presence of 10–30% H<sub>2</sub>O in syngas with a 1:1 H<sub>2</sub>/CO ratio does not significantly influence the CO conversion using a fixed bed reactor. In contrast, Satterfield et al.<sup>93</sup> proposed that cofeeding H<sub>2</sub>O accelerates the deactivation of Fe-based catalysts in slurry-phase FTS when the H<sub>2</sub>/CO ratio is 0.96. However, in the case of a H<sub>2</sub>/CO ratio of 0.52, the cofeeding of 20% H<sub>2</sub>O exhibits no influence on the FTS reaction rate. These studies show that the different roles of H<sub>2</sub>O can be attributed to the difference in reactor type, amount of H<sub>2</sub>O, H<sub>2</sub>/CO ratio, and catalysts used.<sup>94</sup>

Similar to the case for the Co-based catalysts, a promotional role of water has been observed for FTS on Ru catalysts. Hibbitts et al.<sup>89</sup> have shown that with increasing H<sub>2</sub>O pressure, the CO consumption rate and C<sub>5+</sub> selectivity increase continuously, whereas the CH<sub>4</sub> selectivity decreases, as shown in Figure 3b-i. H<sub>2</sub>O can significantly reduce the energy barrier of H-assisted C–O dissociation by facilitating H-transfer (Figure 3a, right). From DFT calculations, in the absence of H<sub>2</sub>O, the kinetically relevant H-transfer step is the formation of the \*HCOH\* intermediate, which follows the formation of HCO\* (formyl route). In this case, the barrier for HCO\* formation is lower than that for \*HCOH\* formation (see Figure 3b-ii), resulting in a first-order H<sub>2</sub> dependence, which is in good agreement with experimental kinetic measurements. In contrast, in the presence of H<sub>2</sub>O, the barrier for the H<sub>2</sub>O-mediated path via the COH\* (hydroxymethyldyne route) is lower than its counterpart in the formyl route (Figure 3b-iii). This reduced energy barrier accelerates the formation of activated C<sub>1</sub> species on the surface and, consequently, the overall rate.

In addition to theoretical simulations, recent development of *in situ/operando* characterization techniques enables a fundamental understanding of the catalytic process under real working conditions at different scales. For example, using magnetic resonance imaging (MRI), Zheng et al.<sup>95</sup> reported the distribution of liquid products and water molecules during FTS on a Ru/TiO<sub>2</sub> catalyst in a pilot fixed-bed reactor. Spatially resolved maps show that the product distribution

becomes broad with a decreasing H<sub>2</sub>/CO feed ratio. The observation of a higher concentration of heavier hydrocarbon chains within the catalyst pores than in the product wax confirms the effect of mass transfer on the overall catalytic process. Furthermore, *operando* two-dimensional MRI spectroscopy indicates that H<sub>2</sub>O in the reactor accumulates on the surface of the pores of the catalyst, forming a water-rich local environment that influences the catalytic performance. Recently, Xu et al.<sup>96</sup> reported the enhanced selectivity toward liquid hydrocarbons in FTS on a bifunctional catalyst composed of a hydrophobic Fe-based catalyst and HZSM-5 zeolite. Molecular dynamic simulations coupled with experiments indicate different diffusion behaviors of H<sub>2</sub>O on the catalyst surfaces with different hydrophilicity/hydrophobicity. On the hydrophilic catalyst, H<sub>2</sub>O can easily reach the iron species encapsulated by the hydrophilic SiO<sub>2</sub> shell, leading to the WGS reaction. In contrast, after hydrophobic functionalization, the hydrophobic SiO<sub>2</sub> shell slows this process and thus prevents the WGS reaction on the Fe surface. As a result, a lower CO<sub>2</sub> selectivity is obtained on the hydrophobically functionalized catalyst with enhanced stability. These results demonstrate that by tuning the surface hydrophilicity/hydrophobicity different structures of H<sub>2</sub>O molecules on the catalyst surface can be achieved to significantly influence the catalytic performance.

On the other hand, the metal-oxide particles can be modified by hydrophobic polymers such as polydimethylsiloxane (PDMS) and polytetrafluoroethylene (PTFE) to obtain hydrophobic materials.<sup>97,98</sup> It has been observed that the catalytic activity of a CoMnC/PDVB catalyst in FTS depends on the manner of mixing of the CoMnC and PDVB components.<sup>99</sup> Compared with a granule mixture (40 to 60 mesh), a powder mixture of the CoMnC and PDVB shows the highest CO conversion of 63.5% and C<sub>2</sub>–C<sub>4</sub> olefin selectivity of 71.4%. The physical mixture of PDVB with CoMnC can modulate the local environment of the catalyst to rapidly remove the H<sub>2</sub>O produced in syngas conversion and shift the H<sub>2</sub>O-adsorption equilibrium on the catalyst surface.<sup>100</sup> Besides introducing hydrophobic substances to change the micro-environment of the active sites on the catalysts, the construction of a hydrophobic shell or functionalization of the catalyst surface with hydrophobicity is also an effective way to suppress side reactions involving H<sub>2</sub>O.<sup>10</sup> For example, the presence of a hydrophobic SiO<sub>2</sub> surface layer in the core–shell FeMn@Si catalyst results in a decrease of the CO<sub>2</sub> selectivity from 45% on the traditional catalyst to about 13%, which is beneficial for the reduction of carbon emissions in FTS.

### 3. H<sub>2</sub>O AS A BYPRODUCT OR PROMOTOR IN HYDROGENATION OF CO<sub>2</sub>

H<sub>2</sub>O is a byproduct in both the direct hydrogenation of CO<sub>2</sub> to methanol (CO<sub>2</sub> + 3H<sub>2</sub> → CH<sub>3</sub>OH + H<sub>2</sub>O) and the main side reaction (reverse water–gas shift reaction: CO<sub>2</sub> + H<sub>2</sub> → CO + H<sub>2</sub>O).<sup>101,102</sup> In some cases, a small amount of H<sub>2</sub>O may also be added to the feed gas as a promoter for methanol synthesis. Both positive and negative effects of H<sub>2</sub>O, either as byproduct or additional feed, on methanol synthesis have been observed, which mainly depend on the nature of the catalysts and the partial pressure of H<sub>2</sub>O. From the perspective of reaction mechanisms, some studies have shown that the H<sub>2</sub>O byproduct might be involved in the reaction through H-transfer, or even participate as an H-source in methanol formation from CO<sub>2</sub> hydrogenation.<sup>7,21,22,103</sup>

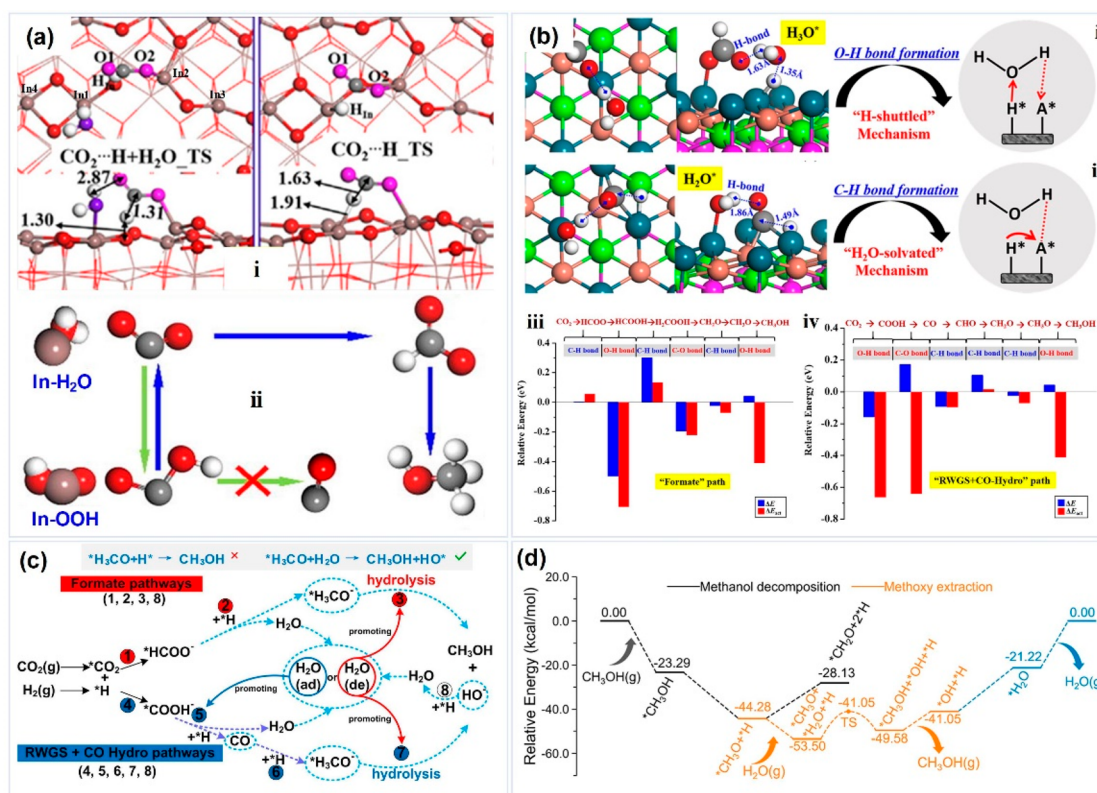


**Figure 4.** (a) Effect of adding H<sub>2</sub>O to the feed gas over In<sub>2</sub>O<sub>3</sub>/ZrO<sub>2</sub> catalysts for CO<sub>2</sub> hydrogenation to methanol: (i) transition state (TS) configurations for HCOO\* formation on an oxygen-defective In<sub>2</sub>O<sub>3</sub>(110) surface in the presence and absence of H<sub>2</sub>O; (ii) schematic illustration of the formation of InOOH species due to H<sub>2</sub>O addition correlating with H<sub>2</sub>O-dependent enhancement of CH<sub>3</sub>OH formation. Reproduced with permission from ref 110. Copyright 2020 Elsevier. (b) Transition state configurations of (i) HCOO\* → HCOOH\* and (ii) CO\* → CHO\* steps involved in CH<sub>3</sub>OH formation with H<sub>2</sub>O included, from which the two “H-transfer” mechanisms are shown for the O–H and C–H bond formation reactions on PdCu(111). Effect of H<sub>2</sub>O on reaction energetics for each elementary step in the (iii) “formate” and (iv) “RWGS+CO-Hydro” paths. ΔE represents the difference in reaction energy between the elementary step with H<sub>2</sub>O and that without H<sub>2</sub>O, and ΔE<sub>act</sub> is defined in the same way but for the activation barrier. Reproduced with permission from ref 21. Copyright 2018 American Chemical Society. (c) Possible pathways of hydrogenation of CO<sub>2</sub> to methanol involving methoxy hydrolysis over Cu-ZnO-ZrO<sub>2</sub> catalysts. Reproduced with permission from ref 7. Copyright 2020 Elsevier. (d) DFT-calculated potential energy diagram for CH<sub>3</sub>OH decomposition and methoxy extraction by H<sub>2</sub>O on a Zr<sub>3</sub>O<sub>10</sub>/Cu(111) model surface. Reproduced with permission from ref 112. Copyright 2022 American Chemical Society.

It is generally accepted that CO<sub>2</sub> hydrogenation includes a pathway with a sequence of reactions involving adsorbed H, and direct hydrogenation with adsorbed H species alone is able to accomplish the production of methanol.<sup>102,104</sup> However, Yang et al.<sup>105</sup> observe via hydrogen titration that the direct hydrogenation of formate species involving adsorbed H species alone fails to produce significant quantities of methanol over Cu-based catalysts. They further propose that coadsorbates related to surface oxygen or H<sub>2</sub>O-derived species may be critical to methanol production on Cu. In addition, a DFT investigation shows evidence for H<sub>2</sub>O being involved in the CO<sub>2</sub> hydrogenation process via the H-transfer mechanism, where weakly bonded CO<sub>2</sub> is hydrogenated by one of the H atoms in H<sub>2</sub>O, which facilitates the formation of the *trans*-COOH intermediate that is the RDS in the hydrocarboxyl mechanism.<sup>22</sup> The presence of H<sub>2</sub>O can kinetically enhance the formation of the COOH\* intermediate while formate hydrogenation is negligible or suppressed.<sup>106</sup> Similarly, a theoretical study over the PdCu<sub>3</sub>(111) surface shows that the coadsorption of H<sub>2</sub>O not only enhances the adsorption of intermediates involved in the RDS but also lowers the activation barrier with the hydrogenation pathway following CO<sub>2</sub>\* → *trans*-COOH\* → *t,t*-COHOH\* → *t,c*-COHOH\* → *c,c*-COHOH\* → COH\* → HCOH\* → H<sub>2</sub>COH\* →

H<sub>3</sub>COH\*.<sup>107</sup> In addition, the energy barrier of CO<sub>2</sub> hydrogenation to methanol can be reduced through the addition of a suitable amount of H<sub>2</sub>O due to the enhanced conversion of the relatively stable intermediates of COOH\* and CH<sub>2</sub>O\*.<sup>108</sup>

In the case of In-based catalysts, formate is considered to be a key intermediate in the hydrogenation of CO<sub>2</sub> to methanol, and the reaction mechanism can be understood as a hydride-proton transfer mechanism.<sup>109,110</sup> In the initial step of HCOO\* formation, one H<sub>2</sub>O molecule is placed on the In<sub>1</sub> site coadsorbed with a hydrogen atom (Figure 4a-i).<sup>110</sup> In the presence of H<sub>2</sub>O, H\* interacts with surface O to form OOH\* due to spatial and electronic effects, which reacts with CO<sub>2</sub> to produce the C–H bond (Figure 4a-ii). While H<sub>2</sub>O does not participate in the H-transfer process, the hydrogenation barrier is reduced by about 31% due to the presence of H<sub>2</sub>O. Consequently, the presence of 0.1 mol % H<sub>2</sub>O can reduce the activation barrier of the RDS (H<sub>2</sub>COO\* + H\* ↔ H<sub>2</sub>CO\* + OH\*) in the formate route, resulting in an increased CH<sub>3</sub>OH yield of approximately 24%.

Nie et al.<sup>21</sup> systematically investigate the effect of trace H<sub>2</sub>O coadsorption on each of the major “formate” and “RWGS+CO-hydro” methanol synthesis pathways, and also explore the chemical processes involved in C–O or C–H bond breaking, O–H bond formation, and C–H bond formation

during methanol production (Figure 4b-i,ii). According to the different H-transfer and intermediate binding pathways, H<sub>2</sub>O participation in the H-transfer mechanism is divided into a H-shuttle mechanism and an H-solvation mechanism. The former occurs through surface H\* being transferred to the H<sub>2</sub>O molecule, which simultaneously transfers another H to the adsorbed reaction intermediates to complete the hydrogenation. H<sub>2</sub>O molecules do not need to be adsorbed to the surface, but can be present in the gas phase to stabilize intermediates through hydrogen bonding, e.g., O–H formation and C–O(H) bond breaking, CO<sub>2</sub> → COOH\*, COOH\* → CO\* + OH\*. The latter mechanism occurs through the adsorption of H<sub>2</sub>O molecules by solvation of the nearby adsorbate, and hydrogenation proceeds via the direct transfer of surface H\* to the adsorbate. The “H<sub>2</sub>O-solvation” mechanism applies to all C–H bond formation reactions, such as CO\* → CHO\*, where H<sub>2</sub>O molecules are adsorbed onto the catalyst surface and undergo solvation by hydrogen bonding to the nearby adsorbate. The results of the effect of H<sub>2</sub>O on the kinetic potential of the CO<sub>2</sub> hydrogenation show that in the formate pathway, the H<sub>2</sub>O shuttle mechanism decreases the activation energy barriers for O–H bond formation (HCOO\* → HCOOH\*, CH<sub>3</sub>O\* → CH<sub>3</sub>OH\*) and C–O(H) bond breaking (H<sub>2</sub>COOH\* → CH<sub>2</sub>O\*), while it has little effect on the C–H bond formation step (Figure 4b-iii,iv). H<sub>2</sub>O exhibits a similar phenomenon for several basic steps of the “RWGS+CO-hydro” pathway. It should be emphasized that the selectivity obtained is based on DFT calculations, where the calculated energy potential is typically subject to an error of 0.2 eV. Therefore, it may be more appropriate to state that the two main routes are equally important for the hydrogenation of CO<sub>2</sub> to methanol.

On Cu-based catalysts, the direct hydrogenation of CH<sub>3</sub>O\* exhibits a relatively high barrier, while H<sub>2</sub>O as the hydrogen source can reduce the hydrogenation barrier to almost zero.<sup>111</sup> The presence of H<sub>2</sub>O results in a reduction of the kinetic barriers of the elementary reactions. Further, our previous results over Cu-ZnO-ZrO<sub>2</sub> catalysts indicate that H<sub>2</sub>O produced during CO<sub>2</sub> hydrogenation is a key active species, which tends to hydrolyze methoxy to methanol (Figure 4c).<sup>7</sup> An interconnected 3D ordered macroporous (3DOM) structure can effectively promote the desorption and diffusion of H<sub>2</sub>O among catalyst particles, resulting in high methanol selectivity. Recent theoretical research supports the above findings and highlights that H<sub>2</sub>O plays two important roles in the evolution of methoxy during CO<sub>2</sub> hydrogenation over the ZrO<sub>2</sub>/Cu(111) surface: (i) preventing decomposition of methoxy and formation of methane by reducing the energy barrier of methoxy hydrogenation to methanol and (ii) extracting the adsorbed methoxy to form gaseous methanol (Figure 4d).<sup>112</sup>

An autocatalytic behavior of H<sub>2</sub>O dissociation leading to the formation of its derivatives has also been reported.<sup>113</sup> Under near ambient conditions, H<sub>2</sub>O–OH is the final state, wherein strong hydrogen bonding reduces the energy barrier of H<sub>2</sub>O dissociation. Xu et al.<sup>114</sup> observe that the value of TOF<sub>CH<sub>3</sub>OH</sub> in the presence of surface O\* or OH\* is at least 1 order of magnitude higher than the value on a clean surface. On the Cu(211) surface, unlike Cu(111),<sup>22</sup> the free energy barrier for CO<sub>2</sub> activation via the HCOO\* or COOH\* pathway by molecular H<sub>2</sub>O near the surface is higher than the direct hydrogenation of H atoms on clean and OH- or O-

preadsorbed surfaces. In this case, H<sub>2</sub>O-derived species, i.e., O\* and OH\*, are responsible for the enhanced catalytic activity due to their coadsorption, which can attenuate poisoning by HCOO\* and reduce the energy barriers. The adsorbed O\* on the surface of catalysts can combine with H<sub>2</sub>O to form two hydroxyl groups with a low barrier of 0.09 eV.<sup>115</sup> Then, the formation of the Zn···OH/Cu active phase can significantly improve the rate of methanol synthesis by facilitating two key steps, namely, HCOO\* and CH<sub>3</sub>O\* hydrogenation. The H atom on the hydroxyl group can directly participate in the reaction as a hydrogen source that reacts with CO<sub>2</sub> to form an HCOO\* intermediate.<sup>116</sup>

Based on the above understanding, researchers have synthesized a series of catalysts with hydroxyl-rich surfaces that are an order of magnitude more active for CO<sub>2</sub> hydrogenation than their corresponding hydroxyl-free structures.<sup>117–119</sup> However, it is important to note that the higher the coverage of surface hydroxyl groups, the more favorable the RWGS reaction, which may lead to methane production.<sup>120</sup> The hydroxyl groups on the oxide supports can significantly weaken the metal–support interaction and destabilize the catalyst.<sup>120</sup> Therefore, the coverage of surface hydroxyl groups needs to be controlled in order to balance the distribution of the desired products and the stability of the catalysts.

Similar phenomena have also been observed for the hydrogenation of CO<sub>2</sub> to higher alcohols (C<sub>2+</sub>OH), such as ethanol synthesis (2CO<sub>2</sub> + 6H<sub>2</sub> → C<sub>2</sub>H<sub>5</sub>OH + 3H<sub>2</sub>O). The promotion of C<sub>2+</sub>OH synthesis from CO<sub>2</sub> hydrogenation by small amounts of H<sub>2</sub>O (<1%) has been observed, and D<sub>2</sub>O labeling experiments have shown that water is involved in alcohol formation as a hydrogen source.<sup>121</sup> It has been proposed that H<sub>2</sub>O can protonate methanol, which readily dissociates into a CH<sub>x</sub>\* species that reacts with CO to form CH<sub>3</sub>CO\*, leading to ethanol formation.<sup>121,122</sup>

It should be highlighted that negative effects are also observed when excess H<sub>2</sub>O is present during CO<sub>2</sub> hydrogenation, although there is no precise threshold for the concentration of H<sub>2</sub>O to cause these effects. It has been observed that methanol formation is significantly suppressed by the presence of H<sub>2</sub>O in the feed as the fraction of H<sub>2</sub>O increases from 10% to 30%, which is presumably due to the competitive adsorption on the active sites.<sup>123,124</sup> It is also found that the byproduct H<sub>2</sub>O during methanol synthesis accelerates the crystallization of Cu and ZnO in the catalysts, leading to catalyst deactivation.<sup>125</sup> For In-based catalysts, an excessive amount of byproduct H<sub>2</sub>O can annihilate the oxygen vacancies and sinter In<sub>2</sub>O<sub>3</sub>.<sup>126,127</sup> In addition, in terms of the influence of product concentration on the reaction rate, methanol has a weaker inhibition effect than water.<sup>103</sup> For CO<sub>2</sub> hydrogenation to higher alcohols, further increasing the H<sub>2</sub>O fraction from 1% to 10% leads to a decrease in both CO<sub>2</sub> conversion and C<sub>2+</sub> selectivity.<sup>121</sup> Under this circumstance, hydrophilic and hydrophobic modification of the CO<sub>2</sub> hydrogenation catalyst may suppress the poisoning effect of H<sub>2</sub>O on active sites during product formation.<sup>128,129</sup>

## 4. H<sub>2</sub>O AS A PROMOTOR OR COREACTANT IN CH<sub>4</sub> ACTIVATION

**4.1. Selective Oxidation of CH<sub>4</sub> to Methanol.** The selective oxidation of CH<sub>4</sub> to methanol has attracted extensive interest from researchers, as the reaction is thermodynamically favorable and can be achieved under mild conditions (CH<sub>4</sub> + 0.5O<sub>2</sub> → CH<sub>3</sub>OH). The reaction mechanism has been



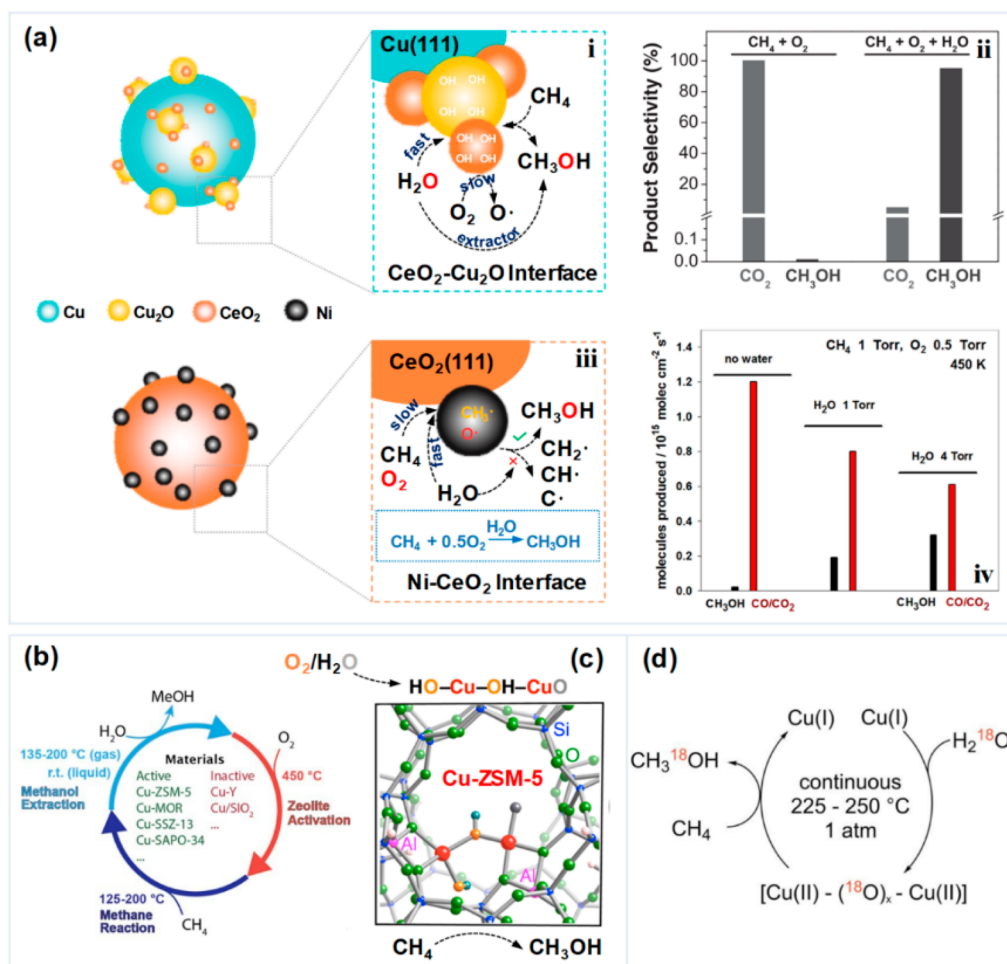


**Figure 5.** (a) The role of H<sub>2</sub>O in interfacial pathways of methane oxidation to methanol over different catalysts: (i) H<sub>2</sub>O-promoted interfacial pathways on a CeO<sub>2</sub>-Cu<sub>2</sub>O catalyst; (ii) selectivity of CH<sub>4</sub> oxidation at 450 K over CeO<sub>2</sub>/Cu<sub>2</sub>O/Cu(111) on exposure to CH<sub>4</sub> and O<sub>2</sub> with a pressure ratio of 2:1 or CH<sub>4</sub>, O<sub>2</sub>, and H<sub>2</sub>O, with a pressure ratio of 2:1:8; (iii) H<sub>2</sub>O-promoted interfacial pathways on a Ni/CeO<sub>2</sub>(111) catalyst; (iv) production of methanol on a Ni/CeO<sub>2</sub>(111) catalyst as a function of H<sub>2</sub>O pressure. The Ni coverage on CeO<sub>2</sub> was ~0.15 ML. The sample was exposed to 1 Torr of CH<sub>4</sub>, 0.5 Torr of O<sub>2</sub>, and 0, 1, or 4 Torr of H<sub>2</sub>O at 450 K. Panel (a)-ii is adapted with permission from ref 140. Copyright 2020 AAAS. Panel (a)-iv is adapted with permission from ref 133. Copyright 2018 American Chemical Society. (b) The discontinuous catalytic conversion of methane to methanol using copper-based molecular sieves. Effect of H<sub>2</sub>O on the selective oxidation of methane to methanol (c) over O<sub>2</sub>-bound Cu-ZSM-5, (d) in a flow reactor over Cu-SSZ-13. Panel (c) is adapted with permission from ref 136. Copyright 2016 American Chemical Society. Panel (d) is adapted with permission from ref 139. Copyright 2020 American Chemical Society.

extensively studied, with a focus on the active site, the nature of reaction intermediates, the reaction pathway, and the role of O<sub>2</sub> in the conversion of CH<sub>4</sub> to CH<sub>3</sub>OH.<sup>130–133</sup> In general, the presence of H<sub>2</sub>O in this reaction can suppress the deep oxidation of methane to CO<sub>2</sub>, improve methane activation, and enhance the desorption of methanol.<sup>133–141</sup>

For example, Rodriguez and co-workers<sup>137</sup> report that methane can be activated at room temperature over a CeO<sub>2</sub>/Cu<sub>2</sub>O/Cu(111) catalyst, forming C, CH<sub>x</sub>, and CO<sub>x</sub> species on the oxide surface, and the OH groups from H<sub>2</sub>O dissociation can saturate the catalyst surface, removing sites that could decompose CH<sub>x</sub> fragments and generating centers on which methane can directly interact to produce methanol. Further studies<sup>140</sup> reveal key steps for the promotion of this reaction by H<sub>2</sub>O on CeO<sub>2</sub>/Cu<sub>2</sub>O/Cu(111), finding that H<sub>2</sub>O can preferentially dissociate at interfacial Ce sites to form OH, as well as inhibit dissociation of O<sub>2</sub>. The active OH\* species can generate CH<sub>3</sub>OH and H\* by reaction with CH<sub>4</sub>\*. In addition, the adsorption of H<sub>2</sub>O is stronger than CH<sub>3</sub>OH, which promotes the desorption of CH<sub>3</sub>OH and increases selectivity

to ~95% (Figure 5a-ii). Briefly, on CeO<sub>2</sub>/Cu<sub>2</sub>O/Cu(111), H<sub>2</sub>O is a key component in the highly selective oxidation of methane to methanol by playing three fundamental roles in interfacial pathways: (i) blocking the possible conversion of methane and methanol to CO or CO<sub>2</sub> at active sites; (ii) providing an oxygen source to participate in the direct conversion of CH<sub>4</sub> → CH<sub>3</sub>OH; and (iii) facilitating the desorption of methanol from the catalyst surface (Figure 5a-i). On ZnO/Cu<sub>2</sub>O/Cu(111),<sup>141</sup> the addition of H<sub>2</sub>O leads to the defective sites on the oxygen-rich ZnO overlay being stably occupied by OH\*, thus hindering the direct oxidation of CH<sub>4</sub> to CO<sub>2</sub> and promoting the extraction of CH<sub>3</sub>O\* as CH<sub>3</sub>OH. Compared to anhydrous conditions, the presence of H<sub>2</sub>O leads to higher methane conversion and enhances the overall methanol selectivity.

Similar to the Cu-based catalysts, on Ni/CeO<sub>2</sub> in the absence of H<sub>2</sub>O, the products are mainly CO/CO<sub>2</sub> and H<sub>2</sub>, while only small amounts of methanol are detected.<sup>133</sup> Methanol selectivity is significantly increased upon addition of H<sub>2</sub>O. In the presence of H<sub>2</sub>O, Ni/CeO<sub>2</sub>(111) exhibits a

different mechanism of direct conversion of methane to methanol than  $\text{CeO}_2/\text{Cu}_2\text{O}/\text{Cu}$  (111) (Figure 5a-iii). The chemisorbed OH and H species from the dissociation of  $\text{H}_2\text{O}$  preferentially occupy the Ni active sites. Thus,  $\text{CH}_3^*$  prefers to react with existing  $\text{O}^*$  species to form  $\text{CH}_3\text{O}^*$ , which is unlikely to decompose on the Ni sites. The optimal coverage of 15% Ni exhibits only about 35% methanol selectivity, which does not change significantly with an increase in  $\text{H}_2\text{O}$  (Figure 5a-iv). Therefore, the role of  $\text{H}_2\text{O}$  on  $\text{CeO}_2/\text{Cu}_2\text{O}/\text{Cu}$  (111) as the main oxygen source that also inhibits the adsorption and dissociation of  $\text{O}_2$  is more significant than its role on Ni/ $\text{CeO}_2$ (111), which involves hindering the dehydrogenation of  $\text{CH}_4$  derivatives ( $\text{CH}_3^*$  or  $\text{CH}_3\text{O}^*$ ).

Inspired by natural methane monooxygenases, molecular sieves loaded with first-row transition metals such as Fe and Cu are considered to be some of the best catalyst candidates for this reaction.<sup>142,143</sup>  $\text{H}_2\text{O}$  also plays an important role in the formation of methanol from methane over Fe- and Cu-exchanged zeolites. Cu-based molecular sieves prepared using ion-exchange methods are the most promising catalysts.<sup>138,144</sup> The concept for the conversion of methane to methanol using such catalysts is shown in Figure 5b. By using active oxygen in zeolites as the oxidant, the oxidation can take place even at room temperature, with few byproducts formed. However, the methanol production rate is influenced by the time required for methanol desorption from  $\text{H}_2\text{O}$ , with a full catalytic cycle typically taking more than 10 h.

At low temperatures (483–498 K), the direct and continuous catalytic oxidation of methane to methanol can be reached using oxygen and  $\text{H}_2\text{O}$  as oxidants on a Cu-exchanged molecular sieve, and  $\text{H}_2\text{O}$  is crucial for methanol formation.<sup>145</sup> Over the  $\text{O}_2$ -bound Cu-ZSM-5 catalyst,<sup>136</sup> H atoms are transferred from the attached  $\text{H}_2\text{O}$  to the bound oxygen molecule to form hydrogen peroxide bridged by a double copper site (Figure 5c). The O–O bond of the peroxyhydrogen species is then cleaved to form oxygen-containing radical intermediates such as  $\text{HO}-\text{Cu}-\text{O}-\text{Cu}-\text{OH}$  and  $\text{HO}-\text{Cu}-\text{OH}-\text{CuO}$ , which both exhibit more efficient methane activation relative to that of  $\text{Cu}-\text{O}-\text{Cu}$  under anhydrous conditions. This mechanism suggests that the coordination effect of  $\text{H}_2\text{O}$  produces active hydroxyl groups that can selectively oxidize methane directly to methanol, but the source of oxygen in methanol is considered to be dioxygen. Similarly, the results of theoretical studies of the selective oxidation of methane to methanol catalyzed by  $\text{H}_2\text{O}$  on Fe/ZSM-5 have shown that  $\text{H}_2\text{O}$  leads to increased activity on the double-coupled  $[\text{Fe}(\mu-\text{O})(\mu-\text{OH})\text{Fe}]^+$  and  $[\text{HOFe}(\mu-\text{O})-\text{FeOH}]^{2+}$  sites compared to the anhydrous sites.<sup>135</sup> Overall, the role of  $\text{H}_2\text{O}$  in the selective oxidation of methane to methanol over Cu- and Fe-based molecular sieve catalysts is mainly to promote the activation of methane and its further selective oxidation to methanol. On the other hand, the oxygen source for methane oxidation to methanol is also proposed to be mainly  $\text{H}_2\text{O}$  rather than  $\text{O}_2$ . Isotope-labeled infrared spectroscopy experiments provide evidence that the oxygen in produced methanol is mainly from the  $\text{H}_2\text{O}$ , as shown in Figure 5d.<sup>139</sup> Likewise, Sun et al.<sup>134</sup> also observed that the presence of  $\text{H}_2\text{O}$  not only induces the reaction but also is the main source of oxygen in the produced methanol, proving that  $\text{H}_2\text{O}$  plays an important role by forming active species for methane activation or participating in the selective oxidation of methane.

**4.2. Steam Reforming of  $\text{CH}_4$ .** Methane is also an important feedstock to produce  $\text{H}_2$ . Currently, over 95% of  $\text{H}_2$  production is accomplished through methane reforming. The steam reforming of methane (SRM,  $\text{CH}_4 + \text{H}_2\text{O} \rightarrow 3\text{H}_2 + \text{CO}$ ) is a predominant industrial process for the production of  $\text{H}_2$  and  $\text{CO}$ , which has been gaining interest.<sup>146</sup> Though this technology was proposed almost 100 years ago, research and industrial efforts to improve catalyst and process design have continued to optimize the reaction system.<sup>147</sup>

The reaction between  $\text{H}_2\text{O}$  and  $\text{CH}_4$  occurs in a high-temperature environment (typically 973–1173 K) and is typically catalyzed by metal-based catalysts.<sup>148</sup> The main pathway of SRM involves the adsorption and dissociation of  $\text{CH}_4$  and  $\text{H}_2\text{O}$  molecules on active metal sites or supports, as well as the subsequent oxidation of carbon-containing intermediates.<sup>149,150</sup> It is generally accepted that the RDS in SRM is the dissociative adsorption of  $\text{CH}_4$ , i.e., cleavage of the C–H bond of  $\text{CH}_4$  that usually occurs on a metal site,<sup>150–152</sup> while  $\text{H}_2\text{O}$  seems play a supporting role.<sup>153–157</sup> For instance, adsorbed OH from  $\text{H}_2\text{O}$  dissociation may assist in the breaking of the first C–H bond in  $\text{CH}_4$ ,<sup>158,157</sup> and the reactive hydroxyl groups are responsible for the further oxidation of carbon-containing intermediates.<sup>159</sup> However, Vogt et al.<sup>160</sup> find that the activation of  $\text{CH}_4$  may not be the only RDS based on isotopically labeled experiments showing the formation of  $\text{CH}_3\text{D}$  upon pulsing  $\text{D}_2\text{O}$ . Their investigation further indicates that, for Ni/ $\text{SiO}_2$  catalysts with relatively large Ni nanoparticles (>4.5 nm), the activation of the  $\text{H}_2\text{O}$  becomes kinetically limiting for SRM.<sup>153,161</sup>

Coking and sintering are two major issues leading to catalyst deactivation in SRM,<sup>147</sup> which are both related to the presence of  $\text{H}_2\text{O}$ . It is generally accepted that  $\text{H}_2\text{O}$  is directly involved in reducing carbon deposition during the SRM reaction.<sup>162,163</sup> In this case, the adsorption of  $\text{H}_2\text{O}$  and oxidation of carbon species by  $\text{H}_2\text{O}$ -derived species play a vital role in carbon suppression.<sup>163,164</sup> A DFT study shows that a MnO–Co catalyst with a strong adsorption capability for  $\text{H}_2\text{O}$  is crucial for inhibiting carbon deposition.<sup>163</sup> In another example, adding  $\text{CeO}_2$  into Rh/ $\text{Al}_2\text{O}_3$  accelerates the reaction between  $\text{H}_2\text{O}$  and carbon species, leading to an enhancement in the overall SRM reaction rates.<sup>164</sup> In addition, the stable conversion rate and product selectivity also depend on the feed ratio of  $\text{H}_2\text{O}/\text{CH}_4$ .<sup>165,166</sup> For a low-temperature SRM on a Ni/ $\text{TiO}_2$  catalyst, a relatively high steam feed ( $\text{H}_2\text{O}:\text{CH}_4 = 3$ ) can effectively drive carbon gasification and stabilize the SRM performance.<sup>165</sup> It should be highlighted that although higher steam feed can effectively reduce the extent of carbon deposition, this strategy may also deactivate catalysts by destroying the internal structure of the support material or leading to the agglomeration of metallic catalyst particles.<sup>165,167</sup> It has been observed that the presence of a hydroxylated Ni surface due to the reaction between  $\text{H}_2\text{O}$  and Ni leads to severe sintering of Ni via Ostwald ripening.<sup>167</sup>

Overall, there should be a balance between the activation of  $\text{CH}_4$  and  $\text{H}_2\text{O}$ . The imbalanced dissociation of  $\text{CH}_4$  and  $\text{H}_2\text{O}$  can induce carbon deposition and metal sintering, and thus lead to the deactivation of Ni catalysts.<sup>168–171</sup> To improve the performance of Ni-based catalysts, many efforts have been made, including the modification of electronic properties of Ni by doping another metal to form a bimetallic structure and the stabilization of Ni nanoparticles by introducing reducible oxide supports,<sup>168,170,172–175</sup> which not only provide active sites for the dissociative adsorption of  $\text{H}_2\text{O}$  but also gasify carbon

deposits. Similar strategies have also been applied to other catalysts to improve their performance for SRM. For example, by performing *in situ* X-ray absorption spectroscopy measurement, Duarte et al.<sup>173</sup> reported that the oxidation state of cerium is partially reduced ( $\text{Ce}^{4+}$  to  $\text{Ce}^{3+}$ ), and Rh is completely reduced for the Rh/CeO<sub>2</sub>-Al<sub>2</sub>O<sub>3</sub> catalyst under SRM conditions. The reduced  $\text{Ce}^{3+}$  reacts with H<sub>2</sub>O and reoxidizes to  $\text{Ce}^{4+}$ , which can readily react with CH<sub>4</sub> to form  $\text{Ce}^{3+}$ . In this way, H<sub>2</sub>O works cooperatively with CeO<sub>2</sub> in the Rh/CeO<sub>2</sub>-Al<sub>2</sub>O<sub>3</sub> catalyst to promote the reaction by altering the oxidation state of CeO<sub>2</sub>, which helps stabilize the Al<sub>2</sub>O<sub>3</sub> structure by forming CeAlO<sub>3</sub> and maintaining the dispersion of the active phase.

It should be highlighted that almost all the above-mentioned mechanisms for SRM are proposed on the basis of experiments performed at relatively low temperatures ( $\leq 873$  K), which are much lower than the industrial operating temperatures ( $> 1073$  K). Since the activations of both H<sub>2</sub>O and CH<sub>4</sub> strongly depend on the reaction temperature, the understanding of reaction mechanisms of SRM under realistic conditions, especially regarding the role of H<sub>2</sub>O, requires further studies. However, experimental investigation of reaction mechanisms at temperatures of  $> 1073$  K is extremely challenging.

**4.3. Oxidative Coupling of CH<sub>4</sub>.** In the oxidative coupling of methane (OCM) reaction, methane can be coupled to produce C<sub>2</sub> hydrocarbons (C<sub>2</sub>H<sub>6</sub> and C<sub>2</sub>H<sub>4</sub>) using O<sub>2</sub> as the oxidant.<sup>176</sup> In contrast to nonoxidative coupling of methane (NOCM), OCM is free from thermodynamic constraints.<sup>177</sup> However, a high operating temperature is still required to activate CH<sub>4</sub> and obtain appreciable C<sub>2</sub> hydrocarbon productivity, which inevitably leads to the further oxidation of the desired products to CO<sub>2</sub>.

The addition of H<sub>2</sub>O is found to result in higher reaction rates and C<sub>2</sub>H<sub>6</sub>/C<sub>2</sub>H<sub>4</sub> yields over the extensively studied MnO<sub>x</sub>-Na<sub>2</sub>WO<sub>4</sub>/SiO<sub>2</sub> catalysts.<sup>178–180</sup> It is proposed that the C–H bond activation can be mediated by either surface atomic oxygen species or surface OH\* radicals originating from H<sub>2</sub>O, which yield CH<sub>3</sub>\* radicals, followed by recombination of the latter to C<sub>2</sub>H<sub>6</sub>. The higher reactivity is suggested to be related to the presence of the more reactive surface OH\* radicals. In addition to accelerating methane conversion, H<sub>2</sub>O can also play a positive role in suppressing the formation of certain surface oxygen species that react with CH<sub>3</sub>\* radicals to produce CO<sub>x</sub>.<sup>181</sup> The presence of H<sub>2</sub>O promotes the dissociation of O<sub>2</sub> on the surface of the catalyst, which suppresses the direct methane oxidation to CO<sub>2</sub> (Figure 6).<sup>182,183</sup>

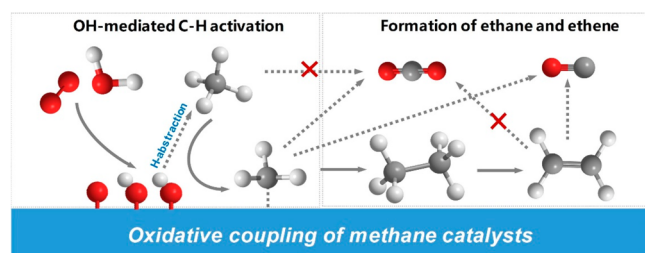


**Figure 6.** H<sub>2</sub>O-mediated pathways for the OCM reaction. Reproduced with permission from ref 182. Copyright 2020 American Chemical Society.

## 5. OUTLOOK AND PERSPECTIVES

In nonaqueous reactions, the presence of H<sub>2</sub>O is often unavoidable, as is the case when H<sub>2</sub>O molecules are present in the reactants (either as an impurity or a coreactant), adsorbed on the surface of catalysts, or formed as a reaction byproduct, etc. As summarized in this Perspective (Figure 7), H<sub>2</sub>O can play important chemical and catalytic roles in the catalytic conversion of C<sub>1</sub> molecules (CO, CO<sub>2</sub> and CH<sub>4</sub>). Some of the positive effects of H<sub>2</sub>O include the following: (i) adsorbing onto the catalyst surface and interacting with reactants to alter the pathway and increase the reaction rate; (ii) decomposing into H\*, OH\*, and O\* species to serve as key intermediates in the conversion process; (iii) forming hydrogen bonds or other noncovalent interactions with reactants to enhance the reactivity and selectivity; (iv) acting as a hydrogen or oxygen source to participate in the reaction.

For catalytic reactions involving CO, H<sub>2</sub>O can be both a reactant and a promoter for H<sub>2</sub> production in the WGS reaction by forming the COOH intermediate, which lowers the reaction energy of the rate-determining step. Similarly, a promotional role of H<sub>2</sub>O has also been proposed for CO oxidation over reducible oxide supported catalysts by facilitating the activation of O<sub>2</sub> and the formation of COOH\*. H<sub>2</sub>O can also participate in the reaction and influence the reaction kinetics in FTS by acting as a proton transfer agent. Over the past few decades, advances in developing *in situ/operando* characterization and computational simulations have improved the molecular-level understanding of the structure and dynamics of H<sub>2</sub>O on solid surfaces. Despite these significant efforts, it remains challenging to experimentally determine the configuration of H<sub>2</sub>O on the catalyst surface under the reaction conditions. Recently, Yuan et al.<sup>184</sup> have reported the structural reconstruction of the anatase TiO<sub>2</sub> surface in the presence of H<sub>2</sub>O and CO using *in situ* environmental TEM. The high spatial and temporal resolution of TEM enables monitoring of the adsorption and dissociation of H<sub>2</sub>O on the TiO<sub>2</sub> surface, which leads to the formation of twinned protrusions that react with CO to form H<sub>2</sub> and CO<sub>2</sub> (WGS). Likewise, ultrafast infrared spectroscopy<sup>185</sup> that probes the stretching mode of the OH group provides opportunities to study the hydrogen bonding dynamics of H<sub>2</sub>O during catalytic reactions.

For the hydrogenation of CO<sub>2</sub>, H<sub>2</sub>O plays a crucial role in methanol synthesis as an important byproduct. H<sub>2</sub>O can play the following three promoting roles in CO<sub>2</sub> hydrogenation reactions: enhancing the formation and further conversion of intermediates via H-transfer, modifying the catalyst surface to form an OH-containing active phase, and promoting the conversion of CH<sub>3</sub>O\* via the hydrolysis reaction. All three roles are related to the presence of H<sub>2</sub>O-derived species (O\*, OH\*, and OOH\*), though details on the reaction pathway are still unclear. Precise identification of the H<sub>2</sub>O-mediated microenvironment on catalysts is still a major challenge in both theoretical and experimental studies. It should be highlighted that the enhancing effects of H<sub>2</sub>O on methanol formation are observed only for systems with trace amounts of H<sub>2</sub>O. Therefore, regulating the conversion of surface intermediates mediated by H<sub>2</sub>O while keeping the active sites and structure of the catalyst unchanged is a major challenge for CO<sub>2</sub> hydrogenation. It is worth emphasizing that H<sub>2</sub>O produced via hydrogenation on the catalyst surface shows a stronger inhibition effect than produced methanol. In this

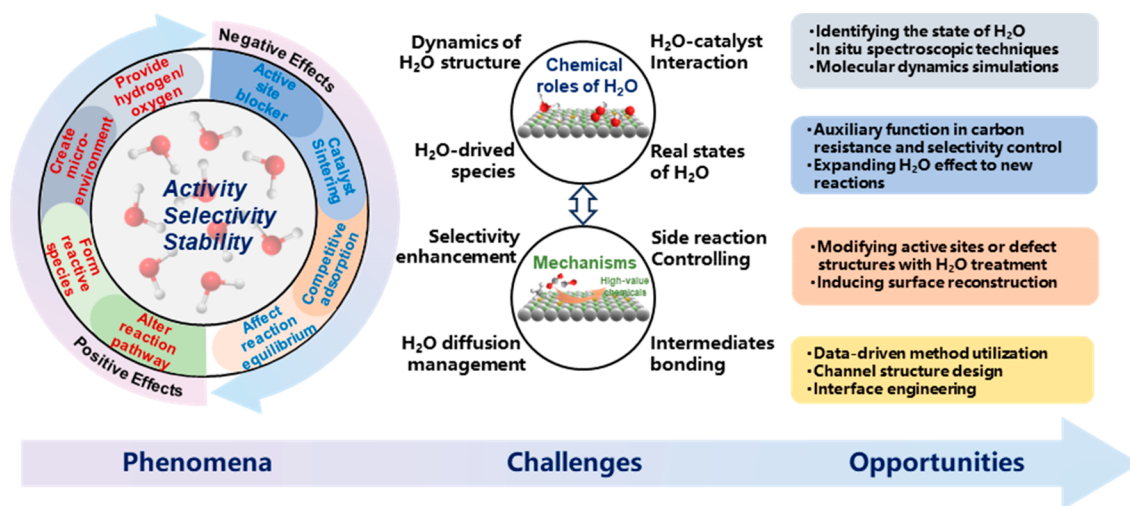


Figure 7. Challenges and opportunities of understanding H<sub>2</sub>O in catalytic conversion of C<sub>1</sub> molecules.

case, both the microscopic point of view to regulate the microenvironment on the surface of the catalyst and the macroscopic point of view to control the chemical equilibrium via enhancing water diffusion are important for designing a high-performance catalyst.

For the catalytic conversion of CH<sub>4</sub> to syngas, methanol, or other hydrocarbons, H<sub>2</sub>O as either a coreactant or a promoter can effectively regulate the selective conversion of CH<sub>4</sub>. H<sub>2</sub>O can promote these reactions from several aspects: creating a weak oxidant atmosphere to avoid the deep oxidation of methane, dissociating at the active sites to form a hydroxyl-rich surface for selective conversion of CH<sub>4</sub>, attenuating the ability of the active site to fully dissociate all of the C–H bonds in CH<sub>4</sub> to avoid carbon deposition on the catalysts, and promoting the desorption of products. Specifically, H<sub>2</sub>O as a weak oxidant can neutralize the strong oxidation effect of oxygen and inhibits the oxidation of methane to CO<sub>2</sub> by producing H<sub>2</sub>O-derived surface reactive oxygen species. For SRM, the presence of H<sub>2</sub>O increases the reaction rate by facilitating the dissociation of CH<sub>4</sub> and promoting surface reactions. It also helps maintain catalyst stability by reducing the formation of carbon deposition on the catalyst surface, while the H<sub>2</sub>O/CH<sub>4</sub> feed ratio is also critical for stabilizing catalytic conversion and product selectivity. Because H<sub>2</sub>O typically adsorbs more strongly than methanol, H<sub>2</sub>O also facilitates the desorption of methanol from the catalyst surface in CH<sub>4</sub> oxidation to methanol. However, a further understanding of the role of H<sub>2</sub>O-derived species in reactions involving the selective conversion of CH<sub>4</sub> is needed to regulate product selectivity during CH<sub>4</sub> conversion by using H<sub>2</sub>O as either a promoter or a reactant.

Although a H<sub>2</sub>O-mediated microenvironment often leads to positive effects in catalytic reactions, direct experimental evidence and detailed explanations of these effects still require further research efforts. In some reactions, H<sub>2</sub>O may also slow the rate, depending on the form and concentration of H<sub>2</sub>O, competitive adsorption mechanisms, and other induced species. In addition to activity and selectivity, the stability of catalysts in the presence of H<sub>2</sub>O, a key parameter of catalytic performance, has not been systematically studied. To better understand and fully exploit the positive effects of H<sub>2</sub>O in gas-phase reactions, more studies should be performed in the following areas:

- (1) *Understanding reaction pathways for H<sub>2</sub>O-mediated conversion of C<sub>1</sub> molecules under realistic conditions.* The combined utilization of *in situ/operando* experimental techniques and theoretical simulations will be critical in understanding the reaction mechanisms and the key steps controlling activity and selectivity. Molecular/atomic-level understanding based on active sites and surface species detected under reaction conditions is essential to design a state-of-art catalyst. At present, the proposed pathways for the involvement of H<sub>2</sub>O in the conversion of C<sub>1</sub> molecules mainly depend on DFT calculations.<sup>6,21,89,186</sup> Most of the H<sub>2</sub>O structures have been observed on clean and well-defined single crystal surfaces under UHV conditions.<sup>187,188</sup> Systematic studies of the structure of H<sub>2</sub>O under ambient/realistic conditions face many difficulties due to the dynamic nature of the interfaces, but represent the next frontier for fundamental research.<sup>189</sup> Future experimental measurements should focus on the identification of active reaction intermediates by *in situ* spectroscopic techniques.<sup>7,116</sup> Meanwhile, more realistic models based on experimental reaction conditions should also be applied to theoretical simulations, for which the combination of kinetic Monte Carlo or molecular dynamics simulations with DFT calculations is necessary.<sup>140</sup> It is noteworthy that the theoretical modeling of H<sub>2</sub>O molecules participating in heterogeneous catalytic reactions in different states should minimize the gap between theory and experiments. Although H<sub>2</sub>O molecules are relatively simple, the presence of molecular forces between them makes it challenging to model them correctly. Therefore, sorting out the various forms of H<sub>2</sub>O (H<sub>2</sub>O molecules, H<sub>2</sub>O clusters, OH/OH, H/H, etc.) and their influence on the energetics of elementary reaction steps is crucial for understanding the reaction mechanisms.
- (2) *Developing characterization techniques to study catalyst surface-H<sub>2</sub>O molecule-intermediate species.* The lack of suitable characterization techniques to identify the structure of solid-H<sub>2</sub>O interfaces, especially *in situ* methods with high spatial and temporal resolution, limits the understanding of catalytic systems in the presence of H<sub>2</sub>O. Traditional surface-sensitive probes,

such as soft X-rays and low-energy electrons, are not capable of penetrating the aqueous layers due to their small mean free path. Therefore, developing experimental methods to identify the interfacial behaviors and elucidate the dynamic processes of H<sub>2</sub>O or H<sub>2</sub>O-derivatives near the solid surface are necessary to enhance understanding. Methods to perform experiments using scanning probe microscope and surface science studies on well-defined model surfaces are of great significance.

- (3) *Investigating stability and selectivity of catalysts under reaction conditions.* Catalyst stability in the presence of H<sub>2</sub>O is one of the critical metrics of catalytic performance in addition to activity and selectivity. For example, experimental and computational studies regarding carbon removal by H<sub>2</sub>O have been performed for decades in the field of methane reforming.<sup>190,191</sup> In addition to inhibiting coking, the presence of H<sub>2</sub>O can also increase the available protons to promote the production of CO and H<sub>2</sub>. Polycyclic aromatics have been shown to be the precursors for coke formation, which causes the deactivation of most zeolite catalysts in C<sub>1</sub> molecule conversion. In the highly selective conversion of CO<sub>2</sub> to aromatics over tandem catalysts, the presence of H<sub>2</sub>O significantly alleviates deactivation of the catalyst by suppressing the formation of these polycyclic aromatics.<sup>192</sup> Moreover, methane dehydroaromatization (MDA) catalysis has potential to replace existing processes due to the increasing global production of natural gas (and biogas). However, the major obstacle for this process is the rapid deactivation of catalysts due to high coke selectivity. The addition of H<sub>2</sub>O has been considered to inhibit coking and improve the lifetime of MDA catalysis in several studies.<sup>193,194</sup> H<sub>2</sub>O plays a vital role in maintaining the activity of heterogeneous catalysts by oxidizing carbon to gas-phase CO or CO<sub>2</sub>. However, as H<sub>2</sub>O concentration increases, the total selectivity of valuable hydrocarbons (aliphatics and aromatics) decreases significantly and CO becomes the dominant product. Therefore, it is important to understand the effect of H<sub>2</sub>O concentration on controlling the catalytic selectivity in these H<sub>2</sub>O-mediated reactions.
- (4) *Enhancing catalytic activity with H<sub>2</sub>O-mediated surface reconstruction of catalysts.* The cocatalysis effect of H<sub>2</sub>O on the catalyst surface is related not only to the reaction system but also to the properties of the catalyst. In some cases, the activity of supported metal nanoparticles depends on their surface structure and exposed sites, and can be promoted by modifying specific types of sites or defect structures.<sup>3,11</sup> For example, steam treatment leading to the formation of twin crystals in Pd-based catalysts for methane catalytic oxidation can increase the grain boundary density and catalytic activity.<sup>195</sup> Such grain boundaries have very high stability, and the reaction rate at the grain boundary sites is 2 orders of magnitude higher than that at the intrinsic catalytic sites on Pd/Al<sub>2</sub>O<sub>3</sub>. Theoretical calculations reveal that the stress formed by the twin crystal defects is the primary factor in the enhanced catalytic activation of the C–H bond. Indeed, double boundaries and grain boundaries are some of the most stable defects on metal surfaces and can act as active sites for some reactions.<sup>195,196</sup>
- Although grain boundaries have been studied as potential defects with catalytic activity, little is known about how they can be generated via interaction with H<sub>2</sub>O. On the other hand, as a byproduct in CO<sub>x</sub> hydrogenation, H<sub>2</sub>O has a strong oxidative and destructive effect on the active phase (Fe<sup>0</sup>/FeC<sub>x</sub>) in Fe-based catalysts, and can also induce oxidation and sintering of the metallic Co phase in FTS.<sup>9,197</sup> The presence of excess H<sub>2</sub>O is detrimental to the stability of carbide catalysts, while moderate amounts can instead enhance their formation and stability.<sup>198</sup> Therefore, it is important to elucidate the positive or negative effects of H<sub>2</sub>O-induced structural changes on catalytic stability and performance in order to rationally modify the synthesis route and reaction atmosphere to optimize the effect of H<sub>2</sub>O.
- (5) *Expanding H<sub>2</sub>O-mediated C<sub>1</sub> conversion to other gaseous phase reactions.* The effect of H<sub>2</sub>O on heterogeneous catalytic systems should be further expanded beyond the conversion of C<sub>1</sub> molecules. It is necessary to develop a systematic understanding of which reactions undergo strong or weak promoter effects due to H<sub>2</sub>O mediation, and to develop a universal basic theory that can be applied to other heterogeneous catalytic reactions. The correlation between H<sub>2</sub>O addition and catalytic activity should be investigated by combining experiments and theory focused on structure–activity relationships.
- (6) *Applying data-driven methods to understand complex roles of H<sub>2</sub>O.* The dynamic nature of H<sub>2</sub>O may also result in its multiple roles in one catalytic system. Quantification of each contribution can be challenging, requiring a combination of experimental kinetic assessments and computational studies. In recent years, the advancement of big data and machine learning (ML) has led to their applications in heterogeneous catalysis.<sup>199</sup> Using theoretical simulations and experimental observations to grow the database and provide guidance for ML training, data-driven ML methods offer additional tools to predict and explain the complex nature and roles of H<sub>2</sub>O-derived species in the catalytic conversion of C<sub>1</sub> molecules.
- (7) *Learning from electrocatalytic studies to further understand the role of H<sub>2</sub>O.* Although the current Perspective focuses on the effects of H<sub>2</sub>O in thermocatalytic reactions, it is important to point out that H<sub>2</sub>O also plays significant roles in electrocatalytic conversion of C<sub>1</sub> molecules, including CO<sub>2</sub>, CO, and methanol. H<sub>2</sub>O is probably the most ubiquitous molecule in electrochemical systems because almost all electrocatalytic reactions occur in aqueous environments, and H<sub>2</sub>O and its dissociated products (OH<sup>−</sup> and H<sup>+</sup>) participate either directly or indirectly in electrochemical reactions involving C<sub>1</sub> molecules. The presence of the water layer at or near the electrocatalysts also modifies the local electrochemical potential that in turn regulates the electrochemical activity and selectivity. Information gained from electrochemical studies should help further elucidate the roles of H<sub>2</sub>O in thermocatalysis.

## AUTHOR INFORMATION

### Corresponding Authors

**Jingguang G. Chen** – Department of Chemical Engineering, Columbia University, New York, New York 10027, United States; [orcid.org/0000-0002-9592-2635](https://orcid.org/0000-0002-9592-2635); Email: [jgchen@columbia.edu](mailto:jgchen@columbia.edu)

**Kongzhai Li** – State Key Laboratory of Complex Nonferrous Metal Resources Clean Utilization Engineering, Kunming University of Science and Technology, Kunming 650093 Yunnan, China; Southwest United Graduate School, Kunming 650000 Yunnan, China; Email: [kongzhai.li@foxmail.com](mailto:kongzhai.li@foxmail.com)

**Gengnan Li** – Center for Nanoscale Materials, Argonne National Laboratory, Lemont, Illinois 60439, United States; Email: [lig@anl.gov](mailto:lig@anl.gov)

### Authors

**Lei Jiang** – State Key Laboratory of Complex Nonferrous Metal Resources Clean Utilization Engineering, Kunming University of Science and Technology, Kunming 650093 Yunnan, China; Faculty of Metallurgical and Energy Engineering, Kunming University of Science and Technology, Kunming 650093 Yunnan, China; [orcid.org/0000-0002-5143-9262](https://orcid.org/0000-0002-5143-9262)

**William N. Porter** – Department of Chemical Engineering, Columbia University, New York, New York 10027, United States; [orcid.org/0000-0002-0908-5317](https://orcid.org/0000-0002-0908-5317)

**Hua Wang** – State Key Laboratory of Complex Nonferrous Metal Resources Clean Utilization Engineering, Kunming University of Science and Technology, Kunming 650093 Yunnan, China

Complete contact information is available at: <https://pubs.acs.org/10.1021/jacs.3c13374>

### Author Contributions

#L.J. and K.L. contributed equally to this work.

### Notes

The authors declare no competing financial interest.

## ACKNOWLEDGMENTS

Authors from Kunming University of Science and Technology acknowledge support from the National Natural Science Foundation of China (Nos. U2202251, 52174279), the Outstanding Youth Project of Yunnan Basic Research Program (No. 202201AV070004), and the Major R&D Special Project of Yunnan Province (No. 202302AG050005). Authors from Columbia University acknowledge support from the U.S. Department of Energy, Office of Basic Energy Sciences, under Contract No. DE-SC0012704. The author from the Argonne National Laboratory acknowledges support from the U.S. Department of Energy, Office of Basic Energy Science, under Contract No. DE-AC02-06CH11357. We thank Dr. Danyang Li of Kunming University of Science and Technology for making contributions to this Perspective.

## REFERENCES

- (1) Ludwig, T.; Gauthier, J. A.; Brown, K. S.; Ringe, S.; Nørskov, J. K.; Chan, K. Solvent-adsorbate interactions and adsorbate-specific solvent structure in carbon dioxide reduction on a stepped Cu surface. *J. Phys. Chem. C* **2019**, *123* (10), 5999–6009.
- (2) Levin, E.; Ivry, E.; Diesendruck, C. E.; Lemcoff, N. G. Water in N-heterocyclic carbene-assisted catalysis. *Chem. Rev.* **2015**, *115* (11), 4607–92.

- (3) Yuan, W.; Zhu, B.; Li, X.-Y.; Hansen, T. W.; Ou, Y.; Fang, K.; Yang, H.; Zhang, Z.; Wagner, J. B.; Gao, Y.; Wang, Y. Visualizing H<sub>2</sub>O molecules reacting at TiO<sub>2</sub> active sites with transmission electron microscopy. *Science* **2020**, *367* (6476), 428–430.

- (4) Merte, L. R.; Peng, G. W.; Bechstein, R.; Rieboldt, F.; Farberow, C. A.; Grabow, L. C.; Kudernatsch, W.; Wendt, S.; Laegsgaard, E.; Mavrikakis, M.; Besenbacher, F. Water-mediated proton hopping on an iron oxide surface. *Science* **2012**, *336* (6083), 889–893.

- (5) Mou, T.; Pillai, H. S.; Wang, S.; Wan, M.; Han, X.; Schweitzer, N. M.; Che, F.; Xin, H. Bridging the complexity gap in computational heterogeneous catalysis with machine learning. *Nat. Catal.* **2023**, *6* (2), 122–136.

- (6) Chang, C. R.; Huang, Z. Q.; Li, J. The promotional role of water in heterogeneous catalysis: mechanism insights from computational modeling. *Wires Comput. Mol. Sci.* **2016**, *6* (6), 679–693.

- (7) Wang, Y.; Gao, W.; Li, K.; Zheng, Y.; Xie, Z.; Na, W.; Chen, J. G.; Wang, H. Strong evidence of the role of H<sub>2</sub>O in affecting methanol selectivity from CO<sub>2</sub> Hydrogenation over Cu-ZnO-ZrO<sub>2</sub>. *Chem.* **2020**, *6* (2), 419–430.

- (8) Wischert, R.; Laurent, P.; Coperet, C.; Delbecq, F.; Sautet, P.  $\gamma$ -Alumina: the essential and unexpected role of water for the structure, stability, and reactivity of "defect" sites. *J. Am. Chem. Soc.* **2012**, *134* (35), 14430–49.

- (9) Wolf, M.; Fischer, N.; Claeys, M. Water-induced deactivation of cobalt-based Fischer–Tropsch catalysts. *Nat. Catal.* **2020**, *3* (12), 962–965.

- (10) Xu, Y.; Li, X.; Gao, J.; Wang, J.; Ma, G.; Wen, X.; Yang, Y.; Li, Y.; Ding, M. A hydrophobic FeMn@Si catalyst increases olefins from syngas by suppressing C1 by-products. *Science* **2021**, *371* (6529), 610–613.

- (11) Li, X.; Wang, X.; Roy, K.; van Bokhoven, J. A.; Artiglia, L. Role of water on the structure of palladium for complete oxidation of methane. *ACS Catal.* **2020**, *10* (10), 5783–5792.

- (12) Wang, Y.; Ma, J.; Wang, X.; Zhang, Z.; Zhao, J.; Yan, J.; Du, Y.; Zhang, H.; Ma, D. Complete CO oxidation by O<sub>2</sub> and H<sub>2</sub>O over Pt-CeO<sub>2-x</sub>/MgO following Langmuir–Hinshelwood and Mars–van Krevelen Mechanisms, Respectively. *ACS Catal.* **2021**, *11* (19), 11820–11830.

- (13) Paulus, U. A.; Wang, Y.; Kim, S. H.; Geng, P.; Wintterlin, J.; Jacobi, K.; Ertl, G. Inhibition of CO oxidation on RuO<sub>2</sub>(110) by adsorbed H<sub>2</sub>O molecules. *J. Chem. Phys.* **2004**, *121* (22), 11301–11308.

- (14) Su, H.-Y.; Yang, M.-M.; Bao, X.-H.; Li, W.-X. The effect of water on the CO oxidation on Ag(111) and Au(111) surfaces: A first-principle study. *J. Phys. Chem. C* **2008**, *112* (44), 17303–17310.

- (15) Xu, X. L.; Li, J. Q. DFT studies on H<sub>2</sub>O adsorption and its effect on CO oxidation over spinel Co<sub>3</sub>O<sub>4</sub> (110) surface. *Surf. Sci.* **2011**, *605* (23–24), 1962–1967.

- (16) Hansen, H. A.; Wolverton, C. Kinetics and thermodynamics of H<sub>2</sub>O dissociation on reduced CeO<sub>2</sub>(111). *J. Phys. Chem. C* **2014**, *118* (47), 27402–27414.

- (17) Liang, Y.; Chen, L.; Ma, C. a. Kinetics and thermodynamics of H<sub>2</sub>O dissociation and CO oxidation on the Pt/WC (0001) surface: A density functional theory study. *Surf. Sci.* **2017**, *656*, 7–16.

- (18) Saavedra, J.; Doan, H. A.; Pursell, C. J.; Grabow, L. C.; Chandler, B. D. The critical role of water at the gold–titania interface in catalytic CO oxidation. *Science* **2014**, *345* (6204), 1599–1602.

- (19) van Spronsen, M. A.; Weststrate, K.-J.; Juurlink, L. B. F. A comparison of CO oxidation by hydroxyl and atomic oxygen from water on low-coordinated Au atoms. *ACS Catal.* **2016**, *6* (10), 7051–7058.

- (20) Mullen, G. M.; Mullins, C. B. Water's place in Au catalysis. *Science* **2014**, *345* (6204), 1564–1565.

- (21) Nie, X.; Jiang, X.; Wang, H.; Luo, W.; Janik, M. J.; Chen, Y.; Guo, X.; Song, C. Mechanistic understanding of alloy effect and water promotion for Pd–Cu bimetallic catalysts in CO<sub>2</sub> hydrogenation to methanol. *ACS Catal.* **2018**, *8* (6), 4873–4892.

- (22) Zhao, Y.-F.; Yang, Y.; Mims, C.; Peden, C. H. F.; Li, J.; Mei, D. Insight into methanol synthesis from CO<sub>2</sub> hydrogenation on

- Cu(111): Complex reaction network and the effects of H<sub>2</sub>O. *J. Catal.* **2011**, *281* (2), 199–211.
- (23) Zhao, Y.-F.; Rousseau, R.; Li, J.; Mei, D. Theoretical study of syngas hydrogenation to methanol on the polar Zn-terminated ZnO(0001) surface. *J. Phys. Chem. C* **2012**, *116* (30), 15952–15961.
- (24) Jiang, X.; Nie, X.; Guo, X.; Song, C.; Chen, J. G. Recent advances in carbon dioxide hydrogenation to methanol via heterogeneous catalysis. *Chem. Rev.* **2020**, *120* (15), 7984–8034.
- (25) Li, G.; Wang, B.; Resasco, D. E. Water-mediated heterogeneously catalyzed reactions. *ACS Catal.* **2020**, *10* (2), 1294–1309.
- (26) Lin, L.; Ge, Y.; Zhang, H.; Wang, M.; Xiao, D.; Ma, D. Heterogeneous Catalysis in Water. *JACS Au* **2021**, *1* (11), 1834–1848.
- (27) Vecchietti, J.; Bonivardi, A.; Xu, W.; Stacchiola, D.; Delgado, J. J.; Calatayud, M.; Collins, S. E. Understanding the role of oxygen vacancies in the water gas shift reaction on ceria-supported platinum catalysts. *ACS Catal.* **2014**, *4* (6), 2088–2096.
- (28) Sun, K.; Kohyama, M.; Tanaka, S.; Takeda, S. Reaction mechanism of the low-temperature water-gas shift reaction on Au/TiO<sub>2</sub> catalysts. *J. Phys. Chem. C* **2017**, *121* (22), 12178–12187.
- (29) Rodriguez, J. A.; Liu, P.; Hrbek, J.; Evans, J.; Perez, M. Water gas shift reaction on Cu and Au nanoparticles supported on CeO<sub>2</sub>(111) and ZnO(0001): intrinsic activity and importance of support interactions. *Angew. Chem., Int. Ed.* **2007**, *46* (8), 1329–1332.
- (30) Gokhale, A. A.; Dumesic, J. A.; Mavrikakis, M. On the mechanism of low-temperature water gas shift reaction on copper. *J. Am. Chem. Soc.* **2008**, *130* (4), 1402–1414.
- (31) Fu, X.-P.; Guo, L.-W.; Wang, W.-W.; Ma, C.; Jia, C.-J.; Wu, K.; Si, R.; Sun, L.-D.; Yan, C.-H. Direct identification of active surface species for the water-gas shift reaction on a gold-ceria catalyst. *J. Am. Chem. Soc.* **2019**, *141* (11), 4613–4623.
- (32) Liang, J. X.; Lin, J.; Liu, J.; Wang, X.; Zhang, T.; Li, J. Dual metal active sites in an Ir<sub>1</sub>/FeO<sub>x</sub> single-atom catalyst: A redox mechanism for the water-gas shift reaction. *Angew. Chem., Int. Ed.* **2020**, *59* (31), 12868–12875.
- (33) Schilling, C.; Hess, C. Elucidating the role of support oxygen in the water-gas shift reaction over ceria-supported gold catalysts using operando spectroscopy. *ACS Catal.* **2019**, *9* (2), 1159–1171.
- (34) Zeinalipour-Yazdi, C. D.; Efstathiou, A. M. Preadsorbed water-promoted mechanism of the water-gas shift reaction. *J. Phys. Chem. C* **2008**, *112* (48), 19030–19039.
- (35) Lin, J.; Wang, A.; Qiao, B.; Liu, X.; Yang, X.; Wang, X.; Liang, J.; Li, J.; Liu, J.; Zhang, T. Remarkable performance of Ir<sub>1</sub>/FeO<sub>x</sub> single-atom catalyst in water gas shift reaction. *J. Am. Chem. Soc.* **2013**, *135* (41), 15314–15317.
- (36) Xu, M.; Yao, S.; Rao, D.; Niu, Y.; Liu, N.; Peng, M.; Zhai, P.; Man, Y.; Zheng, L.; Wang, B.; Zhang, B.; Ma, D.; Wei, M. Insights into interfacial synergistic catalysis over Ni@TiO<sub>2-x</sub> catalyst toward water-gas shift reaction. *J. Am. Chem. Soc.* **2018**, *140* (36), 11241–11251.
- (37) Li, Y.; Kottwitz, M.; Vincent, J. L.; Enright, M. J.; Liu, Z.; Zhang, L.; Huang, J.; Senanayake, S. D.; Yang, W.-C. D.; Crozier, P. A.; Nuzzo, R. G.; Frenkel, A. I. Dynamic structure of active sites in ceria-supported Pt catalysts for the water gas shift reaction. *Nat. Commun.* **2021**, *12* (1), 914.
- (38) Shekhar, M.; Wang, J.; Lee, W. S.; Williams, W. D.; Kim, S. M.; Stach, E. A.; Miller, J. T.; Delgass, W. N.; Ribeiro, F. H. Size and support effects for the water-gas shift catalysis over gold nanoparticles supported on model Al<sub>2</sub>O<sub>3</sub> and TiO<sub>2</sub>. *J. Am. Chem. Soc.* **2012**, *134* (10), 4700–8.
- (39) Liu, N.; Xu, M.; Yang, Y.; Zhang, S.; Zhang, J.; Wang, W.; Zheng, L.; Hong, S.; Wei, M. Au<sup>δ-</sup>-O<sub>v</sub>-Ti<sup>3+</sup> interfacial site: catalytic active center toward low-temperature water gas shift reaction. *ACS Catal.* **2019**, *9* (4), 2707–2717.
- (40) Sun, L.; Xu, J.; Liu, X.; Qiao, B.; Li, L.; Ren, Y.; Wan, Q.; Lin, J.; Lin, S.; Wang, X.; Guo, H.; Zhang, T. High-efficiency water gas shift reaction catalysis on α-MoC promoted by single-atom Ir species. *ACS Catal.* **2021**, *11* (10), 5942–5950.
- (41) Yamamoto, S.; Andersson, K.; Bluhm, H.; Ketteler, G.; Starr, D. E.; Schiros, T.; Ogasawara, H.; Pettersson, L. G. M.; Salmeron, M.; Nilsson, A. Hydroxyl-induced wetting of metals by water at near-ambient conditions. *J. Phys. Chem. C* **2007**, *111* (22), 7848–7850.
- (42) Zhou, L.-L.; Li, S.-Q.; Ma, C.; Fu, X.-P.; Xu, Y.-S.; Wang, W.-W.; Dong, H.; Jia, C.-J.; Wang, F. R.; Yan, C.-H. Promoting molecular exchange on rare-earth oxycarbonate surfaces to catalyze the water-gas shift reaction. *J. Am. Chem. Soc.* **2023**, *145* (4), 2252–2263.
- (43) Zhang, X.; Zhang, M.; Deng, Y.; Xu, M.; Artiglia, L.; Wen, W.; Gao, R.; Chen, B.; Yao, S.; Zhang, X.; Peng, M.; Yan, J.; Li, A.; Jiang, Z.; Gao, X.; Cao, S.; Yang, C.; Kropf, A. J.; Shi, J.; Xie, J.; Bi, M.; van Bokhoven, J. A.; Li, Y.-W.; Wen, X.; Flytzani-Stephanopoulos, M.; Shi, C.; Zhou, W.; Ma, D. A stable low-temperature H<sub>2</sub>-production catalyst by crowding Pt on α-MoC. *Nature* **2021**, *589* (7842), 396–401.
- (44) Yao, S.; Zhang, X.; Zhou, W.; Gao, R.; Xu, W.; Ye, Y.; Lin, L.; Wen, X.; Liu, P.; Chen, B.; Crumlin, E.; Guo, J.; Zuo, Z.; Li, W.; Xie, J.; Lu, L.; Kiely, C. J.; Gu, L.; Shi, C.; Rodriguez, J. A.; Ma, D. Atomic-layered Au clusters on α-MoC as catalysts for the low-temperature water-gas shift reaction. *Science* **2017**, *357* (6349), 389–393.
- (45) Chen, Y.; Lin, J.; Li, L.; Qiao, B.; Liu, J.; Su, Y.; Wang, X. Identifying size effects of Pt as single atoms and nanoparticles supported on FeO<sub>x</sub> for the water-gas shift reaction. *ACS Catal.* **2018**, *8* (2), 859–868.
- (46) Xu, M.; He, S.; Chen, H.; Cui, G.; Zheng, L.; Wang, B.; Wei, M. TiO<sub>2-x</sub>-modified Ni nanocatalyst with tunable metal-support interaction for water-gas shift reaction. *ACS Catal.* **2017**, *7* (11), 7600–7609.
- (47) Liu, N.; Chen, B.; Liu, K.; Qin, R.; Wang, J.; Zhang, Y.; Zhang, Q.; Gu, L.; Liu, P.; Cao, K.; Yan, P.; Fu, G.; Zheng, N. Ensemble effect of the nickel-silica interface promotes the water-gas shift reaction. *ACS Catal.* **2023**, *13* (11), 7347–7357.
- (48) Freund, H. J.; Meijer, G.; Scheffler, M.; Schlögl, R.; Wolf, M. CO oxidation as a prototypical reaction for heterogeneous processes. *Angew. Chem., Int. Ed.* **2011**, *50* (43), 10064–10094.
- (49) Saavedra, J.; Whittaker, T.; Chen, Z.; Pursell, C. J.; Rioux, R. M.; Chandler, B. D. Controlling activity and selectivity using water in the Au-catalyzed preferential oxidation of CO in H<sub>2</sub>. *Nat. Chem.* **2016**, *8* (6), 584–589.
- (50) Bae, J.; Shin, D.; Jeong, H.; Kim, B.-S.; Han, J. W.; Lee, H. Highly water-resistant La-doped Co<sub>3</sub>O<sub>4</sub> catalyst for CO oxidation. *ACS Catal.* **2019**, *9* (11), 10093–10100.
- (51) Wang, H. F.; Kavanagh, R.; Guo, Y. L.; Guo, Y.; Lu, G. Z.; Hu, P. Structural origin: water deactivates metal oxides to CO oxidation and promotes low-temperature CO oxidation with metals. *Angew. Chem., Int. Ed.* **2012**, *51* (27), 6657–61.
- (52) Daté, M.; Haruta, M. Moisture effect on CO oxidation over Au/TiO<sub>2</sub> catalyst. *J. Catal.* **2001**, *201* (2), 221–224.
- (53) Daté, M.; Okumura, M.; Tsubota, S.; Haruta, M. Vital Role of Moisture in the Catalytic Activity of Supported Gold Nanoparticles. *Angew. Chem., Int. Ed.* **2004**, *116* (16), 2181–2184.
- (54) Boccuzzi, F.; Chiorino, A.; Manzoli, M.; Lu, P.; Akita, T.; Ichikawa, S.; Haruta, M. Au/TiO<sub>2</sub> Nanosized Samples: A catalytic, TEM, and FTIR study of the effect of calcination temperature on the CO oxidation. *J. Catal.* **2001**, *202* (2), 256–267.
- (55) Kung, H. H.; Kung, M. C.; Costello, C. K. Supported Au catalysts for low temperature CO oxidation. *J. Catal.* **2003**, *216* (1–2), 425–432.
- (56) Daniells, S. T.; Overweg, A. R.; Makkee, M.; Moulijn, J. A. The mechanism of low-temperature CO oxidation with Au/Fe<sub>2</sub>O<sub>3</sub> catalysts: a combined Mossbauer, FT-IR, and TAP reactor study. *J. Catal.* **2005**, *230* (1), 52–65.
- (57) Kim, T. S.; Gong, J.; Ojifinni, R. A.; White, J. M.; Mullins, C. B. Water activated by atomic oxygen on Au(111) to oxidize CO at low temperatures. *J. Am. Chem. Soc.* **2006**, *128* (19), 6282–6283.
- (58) Ojifinni, R. A.; Froemming, N. S.; Gong, J.; Pan, M.; Kim, T. S.; White, J. M.; Henkelman, G.; Mullins, C. B. Water-enhanced low-temperature CO oxidation and isotope effects on atomic oxygen-covered Au(111). *J. Am. Chem. Soc.* **2008**, *130* (21), 6801–6812.

- (59) Fujitani, T.; Nakamura, I. Mechanism and active sites of the oxidation of CO over Au/TiO<sub>2</sub>. *Angew. Chem., Int. Ed.* **2011**, *50* (43), 10144–10147.
- (60) Li, G.; Li, L.; Yuan, Y.; Shi, J.; Yuan, Y.; Li, Y.; Zhao, W.; Shi, J. Highly efficient mesoporous Pd/CeO<sub>2</sub> catalyst for low temperature CO oxidation especially under moisture condition. *Appl. Catal. B: Environ.* **2014**, *158–159*, 341–347.
- (61) Wang, C.; Gu, X.-K.; Yan, H.; Lin, Y.; Li, J.; Liu, D.; Li, W.-X.; Lu, J. Water-mediated Mars-Van Krevelen mechanism for CO oxidation on ceria-supported single-atom Pt<sub>1</sub> catalyst. *ACS Catal.* **2017**, *7* (1), 887–891.
- (62) Duan, Z.; Henkelman, G. Calculations of CO oxidation over a Au/TiO<sub>2</sub> catalyst: A study of active sites, catalyst deactivation, and moisture effects. *ACS Catal.* **2018**, *8* (2), 1376–1383.
- (63) Schlexer, P.; Widmann, D.; Behm, R. J.; Pacchioni, G. CO oxidation on a Au/TiO<sub>2</sub> nanoparticle catalyst via the Au-assisted Mars-van Krevelen mechanism. *ACS Catal.* **2018**, *8* (7), 6513–6525.
- (64) Zhang, J.; Liu, Y.; Yao, X.; Shao, Q.; Xu, B.; Long, C. Enhanced moisture resistance of Cu/Ce catalysts for CO oxidation via Plasma-Catalyst interactions. *Chemosphere* **2020**, *261*, 127739.
- (65) Dobrosz-Gómez, I.; Kocemba, I.; Rynkowski, J. M. Carbon monoxide oxidation over Au/Ce<sub>1-x</sub>Zr<sub>x</sub>O<sub>2</sub> catalysts: effects of moisture content in the reactant gas and catalyst pretreatment. *Catal. Lett.* **2009**, *128* (3–4), 297–306.
- (66) Ojeda, M.; Zhan, B.-Z.; Iglesia, E. Mechanistic interpretation of CO oxidation turnover rates on supported Au clusters. *J. Catal.* **2012**, *285* (1), 92–102.
- (67) Tran-Thuy, T.-M.; Chen, C.-C.; Lin, S. D. Spectroscopic studies of how moisture enhances CO oxidation over Au/BN at ambient temperature. *ACS Catal.* **2017**, *7* (7), 4304–4312.
- (68) Saavedra, J.; Pursell, C. J.; Chandler, B. D. CO oxidation kinetics over Au/TiO<sub>2</sub> and Au/Al<sub>2</sub>O<sub>3</sub> catalysts: evidence for a common water-assisted mechanism. *J. Am. Chem. Soc.* **2018**, *140* (10), 3712–3723.
- (69) Jin, C.; Zhou, Y.; Han, S.; Shen, W. Water-assisted low-temperature oxidation of CO at the Au-Fe<sub>2</sub>O<sub>3</sub> interface. *J. Phys. Chem. C* **2021**, *125* (47), 26031–26038.
- (70) Deng, Y.; Wang, T.; Zhu, L.; Jia, A.-P.; Lu, J.-Q.; Luo, M.-F. Enhanced performance of CO oxidation over Pt/CuCrO<sub>x</sub> catalyst in the presence of CO<sub>2</sub> and H<sub>2</sub>O. *Appl. Surf. Sci.* **2018**, *442*, 613–621.
- (71) Wang, T.; Xing, J.-Y.; Jia, A.-P.; Tang, C.; Wang, Y.-J.; Luo, M.-F.; Lu, J.-Q. CO oxidation over Pt/Cr<sub>1.3</sub>Fe<sub>0.7</sub>O<sub>3</sub> catalysts: Enhanced activity on single Pt atom by H<sub>2</sub>O promotion. *J. Catal.* **2020**, *382*, 192–203.
- (72) Fujitani, T.; Nakamura, I.; Haruta, M. Role of water in Co oxidation on gold catalysts. *Catal. Lett.* **2014**, *144* (9), 1475–1486.
- (73) Ide, M. S.; Davis, R. J. The important role of hydroxyl on oxidation catalysis by gold nanoparticles. *Acc. Chem. Res.* **2014**, *47* (3), 825–833.
- (74) Jin, Y.; Sun, G.; Xiong, F.; Wang, Z.; Huang, W. Proton-transfer-connected elementary surface reaction network for low-temperature CO oxidation catalyzed by metal-oxide nanocatalysts. *J. Phys. Chem. C* **2016**, *120* (47), 26968–26973.
- (75) Zhao, S.; Chen, F.; Duan, S.; Shao, B.; Li, T.; Tang, H.; Lin, Q.; Zhang, J.; Li, L.; Huang, J.; Bion, N.; Liu, W.; Sun, H.; Wang, A. Q.; Haruta, M.; Qiao, B.; Li, J.; Liu, J.; Zhang, T. Remarkable active-site dependent H<sub>2</sub>O promoting effect in CO oxidation. *Nat. Commun.* **2019**, *10* (1), 3824.
- (76) Iglesia, E. Design, synthesis, and use of cobalt-based Fischer–Tropsch synthesis catalysts. *Appl. Catal. A: Gen.* **1997**, *161* (1), 59–78.
- (77) Rytter, E.; Holmen, A. Perspectives on the effect of water in cobalt Fischer–Tropsch synthesis. *ACS Catal.* **2017**, *7* (8), 5321–5328.
- (78) Yu, X.; Zhang, J.; Wang, X.; Ma, Q.; Gao, X.; Xia, H.; Lai, X.; Fan, S.; Zhao, T.-S. Fischer–Tropsch synthesis over methyl modified Fe<sub>2</sub>O<sub>3</sub>@SiO<sub>2</sub> catalysts with low CO<sub>2</sub> selectivity. *Appl. Catal. B: Environ.* **2018**, *232*, 420–428.
- (79) Dalai, A. K.; Davis, B. H. Fischer–Tropsch synthesis: A review of water effects on the performances of unsupported and supported Co catalysts. *Appl. Catal. A: Gen.* **2008**, *348* (1), 1–15.
- (80) Krishnamoorthy, S.; Tu, M.; Ojeda, M. P.; Pinna, D.; Iglesia, E. An investigation of the effects of water on rate and selectivity for the Fischer–Tropsch synthesis on cobalt-based catalysts. *J. Catal.* **2002**, *211* (2), 422–433.
- (81) Li, J.; Jacobs, G.; Das, T.; Davis, B. H. Fischer–Tropsch synthesis: Effect of water on the catalytic properties of a ruthenium promoted Co/TiO<sub>2</sub> catalyst. *Appl. Catal. A: Gen.* **2002**, *233* (1), 255–262.
- (82) Li, J.; Jacobs, G.; Das, T.; Zhang, Y.; Davis, B. Fischer–Tropsch synthesis: effect of water on the catalytic properties of a Co/SiO<sub>2</sub> catalyst. *Appl. Catal. A: Gen.* **2002**, *236* (1), 67–76.
- (83) Rytter, E.; Tsakoumis, N. E.; Holmen, A. On the selectivity to higher hydrocarbons in Co-based Fischer–Tropsch synthesis. *Catal. Today* **2016**, *261*, 3–16.
- (84) Bertole, C. J.; Mims, C. A.; Kiss, G. The effect of water on the cobalt-catalyzed Fischer–Tropsch synthesis. *J. Catal.* **2002**, *210* (1), 84–96.
- (85) Bertole, C. J.; Mims, C. A.; Kiss, G. Support and rhenium effects on the intrinsic site activity and methane selectivity of cobalt Fischer–Tropsch catalysts. *J. Catal.* **2004**, *221* (1), 191–203.
- (86) Fischer, N.; Clapham, B.; Feltes, T.; Claeys, M. Cobalt-based Fischer–Tropsch activity and selectivity as a function of crystallite size and water partial pressure. *ACS Catal.* **2015**, *5* (1), 113–121.
- (87) Lögdberg, S.; Luaidi, M.; Järäs, S.; Walmsley, J. C.; Blekkan, E. A.; Rytter, E.; Holmen, A. On the selectivity of cobalt-based Fischer–Tropsch catalysts: Evidence for a common precursor for methane and long-chain hydrocarbons. *J. Catal.* **2010**, *274* (1), 84–98.
- (88) Okoye-Chine, C. G.; Moyo, M.; Liu, X.; Hildebrandt, D. A critical review of the impact of water on cobalt-based catalysts in Fischer–Tropsch synthesis. *Fuel Process. Technol.* **2019**, *192*, 105–129.
- (89) Hibbitts, D. D.; Loveless, B. T.; Neurock, M.; Iglesia, E. Mechanistic role of water on the rate and selectivity of Fischer–Tropsch synthesis on ruthenium catalysts. *Angew. Chem., Int. Ed.* **2013**, *52* (47), 12273–8.
- (90) Ojeda, M.; Nabar, R.; Nilekar, A. U.; Ishikawa, A.; Mavrikakis, M.; Iglesia, E. CO activation pathways and the mechanism of Fischer–Tropsch synthesis. *J. Catal.* **2010**, *272* (2), 287–297.
- (91) Pendyala, V. R. R.; Jacobs, G.; Mohandas, J. C.; Luo, M.; Hamdeh, H. H.; Ji, Y.; Ribeiro, M. C.; Davis, B. H. Fischer–Tropsch synthesis: effect of water over iron-based catalysts. *Catal. Lett.* **2010**, *140* (3–4), 98–105.
- (92) Karn, F.; Shultz, J.; Anderson, R. Kinetics of the Fischer–Tropsch synthesis on iron catalysts. III. Influence of water vapour. *Actes Congr. Int. Catal.* **1960**, *2*, 2439.
- (93) Satterfield, C. N.; Hanlon, R. T.; Tung, S. E.; Zou, Z. M.; Papaefthymiou, G. C. Effect of water on the iron-catalyzed Fischer–Tropsch synthesis. *Ind. Eng. Chem. Prod. Res. Dev.* **1986**, *25* (3), 407–414.
- (94) Lin, T.; An, Y.; Yu, F.; Gong, K.; Yu, H.; Wang, C.; Sun, Y.; Zhong, L. Advances in selectivity control for Fischer–Tropsch synthesis to fuels and chemicals with high carbon efficiency. *ACS Catal.* **2022**, *12* (19), 12092–12112.
- (95) Zheng, Q.; Williams, J.; van Thiel, L. R.; Elgersma, S. V.; Mantle, M. D.; Sederman, A. J.; Baart, T. A.; Bezemer, G. L.; Guédon, C. M.; Gladden, L. F. Operando magnetic resonance imaging of product distributions within the pores of catalyst pellets during Fischer–Tropsch synthesis. *Nat. Catal.* **2023**, *6* (2), 185–195.
- (96) Xu, Y.; Liang, H.; Li, R.; Zhang, Z.; Qin, C.; Xu, D.; Fan, H.; Hou, B.; Wang, J.; Gu, X. K.; Ding, M. Insights into the diffusion behaviors of water over hydrophilic/hydrophobic catalysts during the conversion of syngas to high-quality gasoline. *Angew. Chem., Int. Ed.* **2023**, *62* (37), No. e202306786.
- (97) Kamegawa, T.; Shimizu, Y.; Yamashita, H. Superhydrophobic surfaces with photocatalytic self-cleaning properties by nanocompo-



site coating of TiO<sub>2</sub> and polytetrafluoroethylene. *Adv. Mater.* **2012**, *24* (27), 3697–700.

(98) Deng, Z.-Y.; Wang, W.; Mao, L.-H.; Wang, C.-F.; Chen, S. Versatile superhydrophobic and photocatalytic films generated from TiO<sub>2</sub>-SiO<sub>2</sub>@PDMS and their applications on fabrics. *J. Mater. Chem. A* **2014**, *2* (12), 4178–4184.

(99) Fang, W.; Wang, C.; Liu, Z.; Wang, L.; Liu, L.; Li, H.; Xu, S.; Zheng, A.; Qin, X.; Liu, L.; Xiao, F.-S. Physical mixing of a catalyst and a hydrophobic polymer promotes CO hydrogenation through dehydration. *Science* **2022**, *377* (6604), 406–410.

(100) Ding, M.; Xu, Y. Improving catalysis by moving water. *Science* **2022**, *377* (6604), 369–370.

(101) Porosoff, M. D.; Yan, B.; Chen, J. G. Catalytic reduction of CO<sub>2</sub> by H<sub>2</sub> for synthesis of CO, methanol and hydrocarbons: challenges and opportunities. *Energy Environ. Sci.* **2016**, *9* (1), 62–73.

(102) Ye, J.; Liu, C.-j.; Mei, D.; Ge, Q. Methanol synthesis from CO<sub>2</sub> hydrogenation over a Pd<sub>4</sub>/In<sub>2</sub>O<sub>3</sub> model catalyst: A combined DFT and kinetic study. *J. Catal.* **2014**, *317*, 44–53.

(103) Frei, M. S.; Capdevila-Cortada, M.; García-Muelas, R.; Mondelli, C.; López, N.; Stewart, J. A.; Curulla Ferré, D.; Pérez-Ramírez, J. Mechanism and microkinetics of methanol synthesis via CO<sub>2</sub> hydrogenation on indium oxide. *J. Catal.* **2018**, *361*, 313–321.

(104) Jung, K.-D.; Bell, A. T. Role of hydrogen spillover in methanol synthesis over Cu/ZrO<sub>2</sub>. *J. Catal.* **2000**, *193* (2), 207–223.

(105) Yang, Y.; Mims, C. A.; Disselkamp, R. S.; Kwak, J. H.; Peden, C. H. F.; Campbell, C. T. (Non)formation of methanol by direct hydrogenation of formate on copper catalysts. *J. Phys. Chem. C* **2010**, *114* (40), 17205–17211.

(106) Yang, Y.; Mims, C. A.; Mei, D. H.; Peden, C. H. F.; Campbell, C. T. Mechanistic studies of methanol synthesis over Cu from CO/CO<sub>2</sub>/H<sub>2</sub>/H<sub>2</sub>O mixtures: The source of C in methanol and the role of water. *J. Catal.* **2013**, *298*, 10–17.

(107) Liu, L.; Yao, H.; Jiang, Z.; Fang, T. Theoretical study of methanol synthesis from CO<sub>2</sub> hydrogenation on PdCu<sub>3</sub>(111) surface. *Appl. Surf. Sci.* **2018**, *451*, 333–345.

(108) Wu, W.; Wang, Y.; Luo, L.; Wang, M.; Li, Z.; Chen, Y.; Wang, Z.; Chai, J.; Cen, Z.; Shi, Y.; Zhao, J.; Zeng, J.; Li, H. CO<sub>2</sub> hydrogenation over copper/ZnO single-atom catalysts: water-promoted transient synthesis of methanol. *Angew. Chem., Int. Ed.* **2022**, *61* (48), No. e202213024.

(109) Wang, J.; Zhang, G.; Zhu, J.; Zhang, X.; Ding, F.; Zhang, A.; Guo, X.; Song, C. CO<sub>2</sub> hydrogenation to methanol over In<sub>2</sub>O<sub>3</sub>-based catalysts: from mechanism to catalyst development. *ACS Catal.* **2021**, *11* (3), 1406–1423.

(110) Jiang, X.; Nie, X.; Gong, Y.; Moran, C. M.; Wang, J.; Zhu, J.; Chang, H.; Guo, X.; Walton, K. S.; Song, C. A combined experimental and DFT study of H<sub>2</sub>O effect on In<sub>2</sub>O<sub>3</sub>/ZrO<sub>2</sub> catalyst for CO<sub>2</sub> hydrogenation to methanol. *J. Catal.* **2020**, *383*, 283–296.

(111) Tang, Q.-L.; Hong, Q.-J.; Liu, Z.-P. CO<sub>2</sub> fixation into methanol at Cu/ZrO<sub>2</sub> interface from first principles kinetic Monte Carlo. *J. Catal.* **2009**, *263* (1), 114–122.

(112) Rui, N.; Huang, E.; Kim, J.; Mehar, V.; Shi, R.; Rosales, R.; Tian, Y.; Hunt, A.; Waluyo, I.; Senanayake, S. D.; Liu, P.; Rodriguez, J. A. CO<sub>2</sub> hydrogenation to methanol over inverse ZrO<sub>2</sub>/Cu(111) catalysts: The fate of methoxy under dry and wet conditions. *J. Phys. Chem. C* **2022**, *126* (34), 14479–14486.

(113) Andersson, K.; Ketteler, G.; Bluhm, H.; Yamamoto, S.; Ogasawara, H.; Pettersson, L. G. M.; Salmeron, M.; Nilsson, A. Autocatalytic water dissociation on Cu(110) at near ambient conditions. *J. Am. Chem. Soc.* **2008**, *130* (9), 2793–2797.

(114) Xu, D.; Wu, P.; Yang, B. Essential role of water in the autocatalysis behavior of methanol synthesis from CO<sub>2</sub> hydrogenation on Cu: A combined DFT and microkinetic modeling study. *J. Phys. Chem. C* **2019**, *123* (14), 8959–8966.

(115) Wu, X.-K.; Xia, G.-J.; Huang, Z.; Rai, D. K.; Zhao, H.; Zhang, J.; Yun, J.; Wang, Y.-G. Mechanistic insight into the catalytically active phase of CO<sub>2</sub> hydrogenation on Cu/ZnO catalyst. *Appl. Surf. Sci.* **2020**, *525*, 146481–146489.

(116) Peng, Y.; Wang, L.; Luo, Q.; Cao, Y.; Dai, Y.; Li, Z.; Li, H.; Zheng, X.; Yan, W.; Yang, J.; Zeng, J. Molecular-Level Insight into How Hydroxyl Groups Boost Catalytic Activity in CO<sub>2</sub> Hydrogenation into Methanol. *Chem.* **2018**, *4* (3), 613–625.

(117) Song, X.; Yang, C.; Li, X.; Wang, Z.; Pei, C.; Zhao, Z.-J.; Gong, J. On the role of hydroxyl groups on Cu/Al<sub>2</sub>O<sub>3</sub> in CO<sub>2</sub> hydrogenation. *ACS Catal.* **2022**, *12* (22), 14162–14172.

(118) Sha, F.; Tang, S.; Tang, C.; Feng, Z.; Wang, J.; Li, C. The role of surface hydroxyls on ZnZrO solid solution catalyst in CO<sub>2</sub> hydrogenation to methanol. *Chin. J. Catal.* **2023**, *45*, 162–173.

(119) Ye, R.-P.; Ding, J.; Gong, W.; Argyle, M. D.; Zhong, Q.; Wang, Y.; Russell, C. K.; Xu, Z.; Russell, A. G.; Li, Q.; Fan, M.; Yao, Y.-G. CO<sub>2</sub> hydrogenation to high-value products via heterogeneous catalysis. *Nat. Commun.* **2019**, *10* (1), 5698.

(120) Pan, Y.-x.; Liu, C.-j.; Ge, Q. Effect of surface hydroxyls on selective CO<sub>2</sub> hydrogenation over Ni<sub>4</sub>/γ-Al<sub>2</sub>O<sub>3</sub>: A density functional theory study. *J. Catal.* **2010**, *272* (2), 227–234.

(121) He, Z.; Qian, Q.; Ma, J.; Meng, Q.; Zhou, H.; Song, J.; Liu, Z.; Han, B. Water-enhanced synthesis of higher alcohols from CO<sub>2</sub> hydrogenation over a Pt/Co<sub>3</sub>O<sub>4</sub> catalyst under milder conditions. *Angew. Chem., Int. Ed.* **2016**, *55* (2), 737–41.

(122) Yang, C.; Mu, R.; Wang, G.; Song, J.; Tian, H.; Zhao, Z. J.; Gong, J. Hydroxyl-mediated ethanol selectivity of CO<sub>2</sub> hydrogenation. *Chem. Sci.* **2019**, *10* (11), 3161–3167.

(123) Kung, H. H. Deactivation of methanol synthesis catalysts—a review. *Catal. Today* **1992**, *11* (4), 443–453.

(124) Saito, M.; Fujitani, T.; Takeuchi, M.; Watanabe, T. Development of copper/zinc oxide-based multicomponent catalysts for methanol synthesis from carbon dioxide and hydrogen. *Appl. Catal. A: Gen.* **1996**, *138* (2), 311–318.

(125) Wu, J.; Saito, M.; Takeuchi, M.; Watanabe, T. The stability of Cu/ZnO-based catalysts in methanol synthesis from a CO<sub>2</sub>-rich feed and from a CO-rich feed. *Appl. Catal. A: Gen.* **2001**, *218* (1–2), 235–240.

(126) Dang, S.; Qin, B.; Yang, Y.; Wang, H.; Cai, J.; Han, Y.; Li, S.; Gao, P.; Sun, Y. Rationally designed indium oxide catalysts for CO<sub>2</sub> hydrogenation to methanol with high activity and selectivity. *Sci. Adv.* **2020**, *6* (25), No. eaaz2060.

(127) De, S.; Dokania, A.; Ramirez, A.; Gascon, J. Advances in the design of heterogeneous catalysts and thermocatalytic processes for CO<sub>2</sub> utilization. *ACS Catal.* **2020**, *10* (23), 14147–14185.

(128) Li, K.; Chen, J. G. CO<sub>2</sub> Hydrogenation to Methanol over ZrO<sub>2</sub>-Containing Catalysts: Insights into ZrO<sub>2</sub> Induced Synergy. *ACS Catal.* **2019**, *9* (9), 7840–7861.

(129) Xu, D.; Wang, Y.; Ding, M.; Hong, X.; Liu, G.; Tsang, S. C. E. Advances in higher alcohol synthesis from CO<sub>2</sub> hydrogenation. *Chem.* **2021**, *7* (4), 849–881.

(130) Groothaert, M. H.; Smeets, P. J.; Sels, B. F.; Jacobs, P. A.; Schoonheydt, R. A. selective oxidation of methane by the Bis(μ-oxo)dicopper core stabilized on ZSM-5 and mordenite zeolites. *J. Am. Chem. Soc.* **2005**, *127* (5), 1394–1395.

(131) Smeets, P. J.; Hadt, R. G.; Woertink, J. S.; Vanelderen, P.; Schoonheydt, R. A.; Sels, B. F.; Solomon, E. I. Oxygen precursor to the reactive intermediate in methanol synthesis by Cu-ZSM-5. *J. Am. Chem. Soc.* **2010**, *132* (42), 14736–14738.

(132) Li, G.; Vassilev, P.; Sanchez-Sanchez, M.; Lercher, J. A.; Hensen, E. J. M.; Pidko, E. A. Stability and reactivity of copper oxoclusters in ZSM-5 zeolite for selective methane oxidation to methanol. *J. Catal.* **2016**, *338*, 305–312.

(133) Lustemberg, P. G.; Palomino, R. M.; Gutierrez, R. A.; Grinter, D. C.; Vorokhta, M.; Liu, Z.; Ramirez, P. J.; Matolin, V.; Ganduglia-Pirovano, M. V.; Senanayake, S. D.; Rodriguez, J. A. Direct conversion of methane to methanol on Ni-ceria surfaces: Metal-support interactions and water-enabled catalytic conversion by site blocking. *J. Am. Chem. Soc.* **2018**, *140* (24), 7681–7687.

(134) Sun, L.; Wang, Y.; Wang, C.; Xie, Z.; Guan, N.; Li, L. Water-involved methane-selective catalytic oxidation by dioxygen over copper zeolites. *Chem.* **2021**, *7* (6), 1557–1568.

- (135) He, M.; Zhang, J.; Sun, X.-L.; Chen, B.-H.; Wang, Y.-G. Theoretical study on methane oxidation catalyzed by Fe/ZSM-5: The significant role of water on binuclear iron active sites. *J. Phys. Chem. C* **2016**, *120* (48), 27422–27429.
- (136) Yumura, T.; Hirose, Y.; Wakasugi, T.; Kuroda, Y.; Kobayashi, H. Roles of Water Molecules in Modulating the Reactivity of Dioxygen-Bound Cu-ZSM-5 toward Methane: A Theoretical Prediction. *ACS Catal.* **2016**, *6* (4), 2487–2495.
- (137) Zuo, Z.; Ramirez, P. J.; Senanayake, S. D.; Liu, P.; Rodriguez, J. A. Low-temperature conversion of methane to methanol on CeO<sub>x</sub>/Cu<sub>2</sub>O catalysts: water controlled activation of the C-H bond. *J. Am. Chem. Soc.* **2016**, *138* (42), 13810–13813.
- (138) Sushkevich, V. L.; Palagin, D.; Ranocchiaro, M.; van Bokhoven, J. A. Selective anaerobic oxidation of methane enables direct synthesis of methanol. *Science* **2017**, *356* (6337), 523–527.
- (139) Koishybay, A.; Shantz, D. F. Water is the oxygen source for methanol produced in partial oxidation of methane in a flow reactor over Cu-SSZ-13. *J. Am. Chem. Soc.* **2020**, *142* (28), 11962–11966.
- (140) Liu, Z. Y.; Huang, E. W.; Orozco, I.; Liao, W. J.; Palomino, R. M.; Rui, N.; Duchon, T.; Nemsak, S.; Grinter, D. C.; Mahapatra, M.; Liu, P.; Rodriguez, J. A.; Senanayake, S. D. Water-promoted interfacial pathways in methane oxidation to methanol on a CeO<sub>2</sub>-Cu<sub>2</sub>O catalyst. *Science* **2020**, *368* (6490), 513–517.
- (141) Huang, E.; Orozco, I.; Ramirez, P. J.; Liu, Z.; Zhang, F.; Mahapatra, M.; Nemsak, S.; Senanayake, S. D.; Rodriguez, J. A.; Liu, P. Selective methane oxidation to methanol on ZnO/Cu<sub>2</sub>O/Cu(111) catalysts: Multiple site-dependent Behaviors. *J. Am. Chem. Soc.* **2021**, *143* (45), 19018–19032.
- (142) Ross, M. O.; MacMillan, F.; Wang, J.; Nisthal, A.; Lawton, T. J.; Olafson, B. D.; Mayo, S. L.; Rosenzweig, A. C.; Hoffman, B. M. Particulate methane monooxygenase contains only mononuclear copper centers. *Science* **2019**, *364* (6440), 566–570.
- (143) Snyder, B. E. R.; Vanelderen, P.; Bols, M. L.; Hallaert, S. D.; Böttger, L. H.; Ungur, L.; Pierloot, K.; Schoonheydt, R. A.; Sels, B. F.; Solomon, E. I. The active site of low-temperature methane hydroxylation in iron-containing zeolites. *Nature* **2016**, *536* (7616), 317–321.
- (144) Sushkevich, V. L.; Palagin, D.; van Bokhoven, J. A. The effect of the active-site structure on the activity of copper mordenite in the aerobic and anaerobic conversion of methane into methanol. *Angew. Chem., Int. Ed.* **2018**, *57* (29), 8906–8910.
- (145) Narsimhan, K.; Iyoki, K.; Dinh, K.; Roman-Leshkov, Y. Catalytic oxidation of methane into methanol over copper-exchanged zeolites with oxygen at low temperature. *ACS Cent. Sci.* **2016**, *2* (6), 424–429.
- (146) Wismann, S. T.; Engbæk, J. S.; Vendelbo, S. B.; Bendixen, F. B.; Eriksen, W. L.; Aasberg-Petersen, K.; Frandsen, C.; Chorkendorff, I.; Mortensen, P. M. Electrified methane reforming: A compact approach to greener industrial hydrogen production. *Science* **2019**, *364* (6442), 756–759.
- (147) Zhang, H.; Sun, Z.; Hu, Y. H. Steam reforming of methane: Current states of catalyst design and process upgrading. *Renew. Sust. Energy Rev.* **2021**, *149*, 111330.
- (148) Wang, Y.; Xiao, L.; Qi, Y.; Yang, J.; Zhu, Y.-A.; Chen, D. Insight into Size- and Metal-Dependent Activity and the Mechanism for Steam Methane Re-forming in Nanocatalysis. *J. Phys. Chem. C* **2020**, *124* (4), 2501–2512.
- (149) Berman, A.; Karn, R. K.; Epstein, M. Kinetics of steam reforming of methane on Ru/Al<sub>2</sub>O<sub>3</sub> catalyst promoted with Mn oxides. *Appl. Catal. A: Gen.* **2005**, *282* (1–2), 73–83.
- (150) Kechagiopoulos, P. N.; Angeli, S. D.; Lemonidou, A. A. Low temperature steam reforming of methane: A combined isotopic and microkinetic study. *Appl. Catal. B: Environ.* **2017**, *205*, 238–253.
- (151) Roy, S.; Hariharan, S.; Tiwari, A. K. Pt-Ni subsurface alloy catalysts: An improved performance toward CH<sub>4</sub> dissociation. *J. Phys. Chem. C* **2018**, *122* (20), 10857–10870.
- (152) Wei, J. M.; Iglesia, E. Structural and mechanistic requirements for methane activation and chemical conversion on supported iridium clusters. *Angew. Chem., Int. Ed.* **2004**, *43* (28), 3685–3688.
- (153) Wei, J. M.; Iglesia, E. Reaction pathways and site requirements for the activation and chemical conversion of methane on Ru-based catalysts. *J. Phys. Chem. B* **2004**, *108* (22), 7253–7262.
- (154) Wei, J. M.; Iglesia, E. Mechanism and site requirements for activation and chemical conversion of methane on supported Pt clusters and turnover rate comparisons among noble metals. *J. Phys. Chem. B* **2004**, *108* (13), 4094–4103.
- (155) Niu, J. T.; Wang, Y. L.; Qi, Y. Y.; Dam, A. H.; Wang, H. M.; Zhu, Y. A.; Holmen, A.; Ran, J. Y.; Chen, D. New mechanism insights into methane steam reforming on Pt/Ni from DFT and experimental kinetic study. *Fuel* **2020**, *266*, 117143.
- (156) Ke, C.; Lin, Z. Elementary reaction pathway study and a deduced macrokinetic model for the unified understanding of Ni-catalyzed steam methane reforming. *React. Chem. Eng.* **2020**, *5* (5), 873–885.
- (157) Wang, F. F.; Li, Y. J.; Wang, Y. Z.; Zhang, C. X.; Chu, L. Z.; Yang, L. G.; Fan, X. X. Mechanism insights into sorption enhanced methane steam reforming using Ni-doped CaO for H<sub>2</sub> production by DFT study. *Fuel* **2022**, *319*, 123849.
- (158) Wang, H.; Diao, Y.; Gao, Z.; Smith, K. J.; Guo, X.; Ma, D.; Shi, C. H<sub>2</sub> Production from Methane Reforming over Molybdenum Carbide Catalysts: From Surface Properties and Reaction Mechanism to Catalyst Development. *ACS Catal.* **2022**, *12* (24), 15501–15528.
- (159) Matsumura, Y.; Nakamori, T. Steam reforming of methane over nickel catalysts at low reaction temperature. *Appl. Catal. A: Gen.* **2004**, *258* (1), 107–114.
- (160) Vogt, C.; Kranenborg, J.; Monai, M.; Weckhuysen, B. M. Structure sensitivity in steam and dry methane reforming over nickel: Activity and carbon formation. *ACS Catal.* **2020**, *10* (2), 1428–1438.
- (161) Wei, J. M.; Iglesia, E. Structural requirements and reaction pathways in methane activation and chemical conversion catalyzed by rhodium. *J. Catal.* **2004**, *225* (1), 116–127.
- (162) Acha, E.; Requies, J.; Barrio, V. L.; Cambra, J. F.; Güemez, M. B.; Arias, P. L. Water effect in hydrogen production from methane. *Int. J. Hydrog. Energy* **2010**, *35* (20), 11525–11532.
- (163) Fu, Z.; Liu, M.; Sun, Q.; Ma, D.; Yang, Z. Cooperative activation effect on H<sub>2</sub>O adsorption in Mn-Co catalyzed steam methane reforming. *Phys. Lett. A* **2019**, *383* (12), 1357–1361.
- (164) Duarte, R. B.; Olea, M.; Iro, E.; Sasaki, T.; Itako, K.; van Bokhoven, J. A. Transient Mechanistic Studies of Methane Steam Reforming over Ceria-Promoted Rh/Al<sub>2</sub>O<sub>3</sub> Catalysts. *ChemCatChem* **2014**, *6* (10), 2898–2903.
- (165) Kho, E. T.; Scott, J.; Amal, R. Ni/TiO<sub>2</sub> for low temperature steam reforming of methane. *Chem. Eng. Sci.* **2016**, *140*, 161–170.
- (166) Peng, X.; Jin, Q. Molecular simulation of methane steam reforming reaction for hydrogen production. *Int. J. Hydrog. Energy* **2022**, *47* (12), 7569–7585.
- (167) Zhang, X.; Yim, K.; Kim, J.; Wu, D.; Ha, S. Elucidating the promoting role of Mo<sub>2</sub>C in methane activation using Ni-xMo<sub>2</sub>C/FAU to catalyze methane steam reforming. *Appl. Catal. B: Environ.* **2022**, *310*, 121250–121260.
- (168) Carrasco, J.; López-Durán, D.; Liu, Z.; Duchoň, T.; Evans, J.; Senanayake, S. D.; Crumlin, E. J.; Matolín, V.; Rodríguez, J. A.; Ganduglia-Pirovano, M. V. In situ and theoretical studies for the dissociation of water on an active Ni/CeO<sub>2</sub> catalyst: importance of strong metal-support interactions for the cleavage of O-H bonds. *Angew. Chem., Int. Ed.* **2015**, *54* (13), 3917–3921.
- (169) Salcedo, A.; Lustemberg, P. G.; Rui, N.; Palomino, R. M.; Liu, Z.; Nemsak, S.; Senanayake, S. D.; Rodriguez, J. A.; Ganduglia-Pirovano, M. V.; Irigoyen, B. Reaction pathway for coke-free methane steam reforming on a Ni/CeO<sub>2</sub> catalyst: active sites and the role of metal-support interactions. *ACS Catal.* **2021**, *11* (13), 8327–8337.
- (170) Nikolla, E.; Holewinski, A.; Schwank, J.; Linic, S. Controlling carbon surface chemistry by alloying: carbon tolerant reforming catalyst. *J. Am. Chem. Soc.* **2006**, *128* (35), 11354–11355.
- (171) Chen, L.; Qi, Z.; Peng, X.; Chen, J.-L.; Pao, C.-W.; Zhang, X.; Dun, C.; Young, M.; Prendergast, D.; Urban, J. J. Insights into the mechanism of methanol steam reforming tandem reaction over CeO<sub>2</sub>

- supported single-site catalysts. *J. Am. Chem. Soc.* **2021**, *143* (31), 12074–12081.
- (172) Mortola, V.; Damyanova, S.; Zanchet, D.; Bueno, J. Surface and structural features of Pt/CeO<sub>2</sub>-La<sub>2</sub>O<sub>3</sub>-Al<sub>2</sub>O<sub>3</sub> catalysts for partial oxidation and steam reforming of methane. *Appl. Catal. B: Environ.* **2011**, *107* (3–4), 221–236.
- (173) Duarte, R.; Safonova, O.; Krumeich, F.; Makosch, M.; van Bokhoven, J. A. Oxidation state of Ce in CeO<sub>2</sub>-promoted Rh/Al<sub>2</sub>O<sub>3</sub> catalysts during methane steam reforming: H<sub>2</sub>O activation and alumina stabilization. *ACS Catal.* **2013**, *3* (9), 1956–1964.
- (174) Halabi, M.; De Croon, M.; Van Der Schaaf, J.; Cobden, P.; Schouten, J. Intrinsic kinetics of low temperature catalytic methane-steam reforming and water-gas shift over Rh/Ce<sub>α</sub>Zr<sub>1-α</sub>O<sub>2</sub> catalyst. *Appl. Catal. A: Gen.* **2010**, *389* (1–2), 80–91.
- (175) Halabi, M.; De Croon, M.; Van der Schaaf, J.; Cobden, P.; Schouten, J. Low temperature catalytic methane steam reforming over ceria-zirconia supported rhodium. *Appl. Catal. A: Gen.* **2010**, *389* (1–2), 68–79.
- (176) Farrell, B. L.; Igenegbai, V. O.; Lincic, S. A Viewpoint on Direct Methane Conversion to Ethane and Ethylene Using Oxidative Coupling on Solid Catalysts. *ACS Catal.* **2016**, *6* (7), 4340–4346.
- (177) Mesters, C. A Selection of Recent Advances in C1 Chemistry. *Annu. Rev. Chem. Biomol. Eng.* **2016**, *7*, 223–38.
- (178) Takanabe, K.; Iglesia, E. Rate and selectivity enhancements mediated by OH radicals in the oxidative coupling of methane catalyzed by Mn/Na<sub>2</sub>WO<sub>4</sub>/SiO<sub>2</sub>. *Angew. Chem., Int. Ed.* **2008**, *47* (40), 7689–7693.
- (179) Takanabe, K.; Iglesia, E. Mechanistic Aspects and reaction pathways for oxidative coupling of methane on Mn/Na<sub>2</sub>WO<sub>4</sub>/SiO<sub>2</sub> catalysts. *J. Phys. Chem. C* **2009**, *113* (23), 10131–10145.
- (180) Kiani, D.; Sourav, S.; Baltrusaitis, J.; Wachs, I. E. Oxidative Coupling of Methane (OCM) by SiO<sub>2</sub>-Supported Tungsten Oxide Catalysts Promoted with Mn and Na. *ACS Catal.* **2019**, *9* (7), 5912–5928.
- (181) Lomonosov, V.; Gordienko, Y.; Sinev, M. Effect of water on methane and ethane oxidation in the conditions of oxidative coupling of methane over model Catalysts. *Top. Catal.* **2013**, *56* (18–20), 1858–1866.
- (182) Aydin, Z.; Kondratenko, V. A.; Lund, H.; Bartling, S.; Kreyenschulte, C. R.; Linke, D.; Kondratenko, E. V. Revisiting activity- and selectivity-enhancing effects of water in the oxidative coupling of methane over MnO<sub>x</sub>-Na<sub>2</sub>WO<sub>4</sub>/SiO<sub>2</sub> and proving for other materials. *ACS Catal.* **2020**, *10* (15), 8751–8764.
- (183) Aydin, Z.; Zanina, A.; Kondratenko, V. A.; Rabeah, J.; Li, J.; Chen, J.; Li, Y.; Jiang, G.; Lund, H.; Bartling, S.; Linke, D.; Kondratenko, E. V. Effects of N<sub>2</sub>O and Water on Activity and Selectivity in the Oxidative Coupling of Methane over Mn-Na<sub>2</sub>WO<sub>4</sub>/SiO<sub>2</sub>: Role of Oxygen Species. *ACS Catal.* **2022**, *12* (2), 1298–1309.
- (184) Yuan, W.; Zhu, B.; Li, X.-Y.; Hansen, T. W.; Ou, Y.; Fang, K.; Yang, H.; Zhang, Z.; Wagner, J. B.; Gao, Y.; Wang, Y. Visualizing H<sub>2</sub>O molecules reacting at TiO<sub>2</sub> active sites with transmission electron microscopy. *Science* **2020**, *367* (6476), 428–430.
- (185) Fayer, M. D. Dynamics of water interacting with interfaces, molecules, and ions. *Acc. Chem. Res.* **2012**, *45* (1), 3–14.
- (186) Graciani, J.; Grinter, D. C.; Ramirez, P. J.; Palomino, R. M.; Xu, F.; Waluyo, I.; Stacchiola, D.; Fdez Sanz, J.; Senanayake, S. D.; Rodriguez, J. A. Conversion of CO<sub>2</sub> to methanol and ethanol on Pt/CeO<sub>x</sub>/TiO<sub>2</sub>(110): enabling role of water in C-C bond formation. *ACS Catal.* **2022**, *12* (24), 15097–15109.
- (187) Mu, R.; Zhao, Z.-j.; Dohnálek, Z.; Gong, J. Structural motifs of water on metal oxide surfaces. *Chem. Soc. Rev.* **2017**, *46* (7), 1785–1806.
- (188) Shiotari, A.; Sugimoto, Y. Ultrahigh-resolution imaging of water networks by atomic force microscopy. *Nat. Commun.* **2017**, *8* (1), 14313.
- (189) Qu, J.; Sui, M.; Li, R. Recent advances in in-situ transmission electron microscopy techniques for heterogeneous catalysis. *iScience* **2023**, *26* (7), 107072.
- (190) Pakhare, D.; Spivey, J. A review of dry (CO<sub>2</sub>) reforming of methane over noble metal catalysts. *Chem. Soc. Rev.* **2014**, *43* (22), 7813–7837.
- (191) Salcedo, A.; Lustemberg, P. G.; Rui, N.; Palomino, R. M.; Liu, Z.; Nemsak, S.; Senanayake, S. D.; Rodriguez, J. A.; Ganduglia-Pirovano, M. V.; Irigoyen, B. Reaction pathway for coke-free methane steam reforming on a Ni/CeO<sub>2</sub> catalyst: Active Sites and the role of metal-support interactions. *ACS Catal.* **2021**, *11* (13), 8327–8337.
- (192) Li, Z.; Qu, Y.; Wang, J.; Liu, H.; Li, M.; Miao, S.; Li, C. Highly selective conversion of carbon dioxide to aromatics over tandem catalysts. *Joule* **2019**, *3* (2), 570–583.
- (193) Liu, S. L.; Ohnishi, R.; Ichikawa, M. Promotional role of water added to methane feed on catalytic performance in the methane dehydroaromatization reaction on Mo/HZSM-5 catalyst. *J. Catal.* **2003**, *220* (1), 57–65.
- (194) Çağlayan, M.; Paioni, A. L.; Dereli, B.; Shterk, G.; Hita, I.; Abou-Hamad, E.; Pustovarenko, A.; Emwas, A.-H.; Dikhtiarrenko, A.; Castaño, P.; Cavallo, L.; Baldus, M.; Chowdhury, A. D.; Gascon, J. Illuminating the Intrinsic effect of water co-feeding on methane dehydroaromatization: A comprehensive study. *ACS Catal.* **2021**, *11* (18), 11671–11684.
- (195) Huang, W.; Johnston-Peck Aaron, C.; Wolter, T.; Yang Wei-Chang, D.; Xu, L.; Oh, J.; Reeves Benjamin, A.; Zhou, C.; Holtz Megan, E.; Herzing Andrew, A.; Lindenberg Aaron, M.; Mavrikakis, M.; Cargnello, M. Steam-created grain boundaries for methane C-H activation in palladium catalysts. *Science* **2021**, *373* (6562), 1518–1523.
- (196) Polo-Garzon, F.; Bao, Z.; Zhang, X.; Huang, W.; Wu, Z. Surface Reconstructions of Metal Oxides and the Consequences on Catalytic Chemistry. *ACS Catal.* **2019**, *9* (6), 5692–5707.
- (197) Zhu, J.; Wang, P.; Zhang, X. B.; Zhang, G. H.; Li, R. T.; Li, W. H.; Senftle, T. P.; Liu, W.; Wang, J. Y.; Wang, Y. L.; Zhang, A. F.; Fu, Q.; Song, C. S.; Guo, X. W. Dynamic structural evolution of iron catalysts involving competitive oxidation and carburization during CO<sub>2</sub> hydrogenation. *Sci. Adv.* **2022**, *8* (5), No. eabm3629.
- (198) Wang, M.; Wang, P.; Zhang, G.; Cheng, Z.; Zhang, M.; Liu, Y.; Li, R.; Zhu, J.; Wang, J.; Bian, K.; Liu, Y.; Ding, F.; Senftle, T. P.; Nie, X.; Fu, Q.; Song, C.; Guo, X. Stabilizing CO<sub>2</sub>C with H<sub>2</sub>O and K promoter for CO<sub>2</sub> hydrogenation to C<sub>2+</sub> hydrocarbons. *Sci. Adv.* **2023**, *9* (24), No. eadg0167.
- (199) Li, H.; Jiao, Y.; Davey, K.; Qiao, S. Z. Data-driven machine learning for understanding surface structures of heterogeneous catalysts. *Angew. Chem.Int. Ed.* **2023**, *62* (9), No. e202216383.